

## Computational Design, Spectral, NBO, DOS, Bioactivity Evaluation, ADMET Analysis, Third-Order non-linear Optical and Quantum Chemical Investigations on Hydrogen Bonded Novel Organic Molecular Complex of 4-[Bis[2-(acetyloxy)ethyl]amino]benzaldehyde (4B2AEAB) Derivatives for Opto-Electronic Applications

ASHUTOSH KUMAR<sup>1</sup> and ANIL MISHRA<sup>\*1</sup>

Department of Chemistry, University of Lucknow, Lucknow-226007, India

\*Corresponding author: E-mail: [mishraanil101@hotmail.com](mailto:mishraanil101@hotmail.com); [ashutosh.chemist@gmail.com](mailto:ashutosh.chemist@gmail.com)

Received: 21 May 2020;

Accepted: 18 July 2020;

Published online: 28 October 2020;

AJC-20103

In this paper, the authors reported a theoretical investigation on molecular structure, geometry optimization, global and local chemical reactivity descriptors calculations, NBO study, DOS, non-linear optical behaviour and vibrational wavenumbers of the novel 4-[bis[2-(acetyloxy)ethyl]amino]benzaldehyde (4B2AEAB) were carried out by DFT (B3LYP and B3PW91) methods with 6-31+G (d, p) basis set in water solvent. The calculated vibrational wavenumbers are found to be in good agreement with experimental FT-IR spectra and PED analysis using GaussView 5.0 and VEDA 4 program. The UV-Vis absorption spectrum of 4B2AEAB was calculated by using TD-DFT/B3LYP/6-31+G(d,p) in gas phase, water, CHCl<sub>3</sub>, DMSO and CH<sub>2</sub>Cl<sub>2</sub> solvents using CPCM model and  $\lambda_{max}$  in range of 354.16, 341.35, 343.74, 342.18 and 342.64 nm, respectively. The density of state (DOS spectrum) of the compound in term of HOMOs and LUMOs and MESP were calculated and analyzed. The temperature effects on the thermodynamic properties are also discussed. The calculated <sup>1</sup>H NMR and <sup>13</sup>C NMR chemical shift using GIAO method and solvent effect are investigated by B3LYP/6-31+G(d,p) in gas phase, chloroform, water, DMSO and CH<sub>2</sub>Cl<sub>2</sub> solvents and correlate with experimental chemical shifts. The dipole moment, polarizability and the first static hyperpolarizability values show that the 4B2AEAB molecule is active non-linear optical (NLO) material. The nucleophilic and electrophilic reactive sites in the 4B2AEAB and its derivatives were analyzed by Fukui function analysis using Mulliken charge. The charge transfer, conjugative interactions and delocalization of electron density are analyzed by natural bond orbital (NBO) analysis. The biological properties and ADMET study of 4B2AEAB and its derivatives are also discussed.

**Keywords:** Molecular structure, DFT/TD-DFT, Spectroscopic properties, Non-linear optics, NBO, ADMET analysis.

### INTRODUCTION

In last two decades, rational designing of new compounds with desired properties is essential to the study of non-linear optical (NLO) materials with quadratic response in presence of electromagnetic field have been performed and become advance field of multidisciplinary research after the discovery of laser. The non-linear optical materials play important role in the field of optoelectronics and photonics and have potential applications in the areas like optical limiting, laser radiation protection, optical logic gates, optical signature processing, optical switching, harmonic generation, optical storage, optical communication, optical computing, dynamic holography, frequency mixing, *etc.* [1-3]. Moreover, organic materials with

extensively delocalized  $\pi$ -electrons have received important attention because of their massive NLO condition, field of study flexibility and simple fabrication of NLO devices [4-8]. Current research reveals that the organic NLO (non-linear optical) materials are used for developing relatively low-power laser-driven non-linear optical system. The organic non-linear optical materials exhibit quick optical response time, large non-linear optical coefficient but high second harmonic generation (SHG) efficiency, compared to inorganic materials [9,10], to obtain the required structure and therefore the value effects are the special options of organic materials. Non-linear optical effects in organic compounds are very large as compared to inorganic compounds. This is because they have strong donor-acceptor intermolecular interactions as well as delocalized  $\pi$ -

electrons systems, in addition to organic materials due to flexible nature, could crystallize in a centrosymmetric (CS) or non centrosymmetric (NCS) manner with unidirectional oriented dipole moments and ability to get dissolved in various solvents [11-14]. The non-linearity in organic materials is generally governed by the nature of  $\pi$ -bonding sequence (donor-acceptor groups), conjugation length. The NLO properties are directly related to linear polarizability ( $\alpha$ ), the second order hyperpolarizability ( $\beta$ ) and the third order hyperpolarizability ( $\gamma$ ) arises usually from  $\pi$ -conjugated donor-acceptor groups [15-20]. Further, from the literature survey, it is observed that the intermolecular or adduct type non-linear optical materials are crystallized in various hydrated, anhydrous and solvents. Many combinations of thiourea, phenolate, benzoate, pyridine and aldehyde related organic materials given the literature and has explored extensively for their efficacious non-linear optical (NLO) properties [21-29]. The inter-molecular or hydrogen bonded, adduct and aldehyde related NLO materials such as 4-(dimethylamino) benzaldehyde [30], thiourea 4-(dimethyl-amino)benzaldehyde [31], 4-dimethylamino benzaldehyde 4-nitrophenol [32], 4-chloro-3-nitroaniline-3-hydroxybenzaldehyde and other inter-molecular NLO materials like 4-acetylanilinium dihydrogen phosphate (4AADP) [33], urea-4-dimethyl-aminopyridine [33] are given in the literature. In present study, we have rationally designed that three novel NLO materials namely 4-[bis[2-(acetyloxy)ethyl]amino]benzaldehyde (4B2AEAB), O—H—O hydrogen bonded 4-[bis[2-(acetyloxy)-ethyl]amino]benzaldehyde 4-nitrophenol (4B2AEAB4NP), 4-[bis[2-(acetyloxy)-ethyl]amino]benzaldehyde thiourea (4B2AEABTU). Naem *et al.* [34] reported that various charge transfer phenomena in 4-(dimethylamino)benzaldehyde (electron donor) and 4-nitrophenol (electron acceptor) complex. Herein, 4-nitrophenol and its derivatives are promising NLO materials typical example of D- $\pi$ -A (donor- $\pi$ -acceptor) system [35]. Herein, we also used thiourea ( $\text{CH}_4\text{N}_2\text{S}$ ) as an organic compound, which has orthorhombic crystal structure system with centrosymmetric, Pnma, space group [36]. Thiourea has intermolecular charge transfer (ICT) property within the molecule because contains both electron acceptor and withdrawing groups. The interesting property of ICT causes enhancement of NLO response while combining with both organic molecules. Herein, we are searching new organic non-linear optical (NLO) materials for the design of applications of optoelectronic devices. Here, we are studied three novel NLO materials such as 4-[bis[2-(acetyloxy)ethyl]amino]benzaldehyde (4B2AEAB) and remaining two hydrogen bonded 4-[bis[2-(acetyloxy)ethyl]amino]benzaldehyde 4-nitrophenol (4B2AEAB4NP) and 4-[bis[2-(acetyloxy)ethyl]amino]benzaldehyde thiourea (4B2AEABTU).

In this paper, we present the spectroscopic properties such as vibrational spectra (IR),  $^1\text{H}$  &  $^{13}\text{C}$  NMR chemical shifts, UV-visible spectral parameters, molecular geometrical properties, NBO analysis, atomic charges, HOMO and LUMO properties, DOS spectrum, MESP, NLO properties and temperature effect on thermodynamic properties of 4-[bis[2-(acetyloxy)-ethyl]amino]benzaldehyde (4B2AEAB) molecule. The theoretical spectroscopic investigations well supported by experi-

mental method taken from literature. The quantum chemical investigations were performed by means of DFT/B3LYP and DFT/B3PW91 method with the 6-31+G(d,p) basis set. The comparative analysis of non-linear optical (NLO) properties of 4B2AEAB molecule and its derivatives are discussed. We are also investigate the *in silico* biological properties and ADME/T analysis in detail. Additionally, the quantum chemical computations provide a more satisfactory results and powerful support for theoretical studies.

## EXPERIMENTAL

**Structure and spectra:** The optimized molecular structure of 4-[bis[2-(acetyloxy)ethyl]amino]benzaldehyde (4B2AEAB) and its derivatives (4B2AEAB4NP and 4B2AEABTU) is shown in Fig. 1. The experimental FT-IR spectrum wavenumbers of 4B2AEAB molecule is conducted to in the range of 4000-400  $\text{cm}^{-1}$  with spectral resolution of 4  $\text{cm}^{-1}$  and found to match well with theoretically calculated wavenumbers in water solvent. The experimental FT-IR,  $^1\text{H}$  and  $^{13}\text{C}$  NMR spectra in  $\text{CDCl}_3$  solvent of 4B2AEAB molecule are reported at Sigma-Aldrich website [37].

**Computational details:** The DFT computations of geometry optimization, IR wavenumbers (using B3LYP and B3PW91 method in water solvent),  $^1\text{H}$  and  $^{13}\text{C}$  NMR chemical shifts (using B3LYP method in  $\text{CHCl}_3$ , gas, water, DMSO and DCM), UV-visible spectroscopic parameters (using B3LYP method in water, DMSO, DCM,  $\text{CHCl}_3$  and gas phase), global and local properties analyses, NBO study, NLO properties, atomic charges, FMOs analyses and temperature effect on thermodynamic properties analysis of 4B2AEAB molecule and its derivatives were done using Gaussian 09 Revision-A02 program package [38]. The theoretically calculated results were visualized by *via* Gauss View 5.0.8 program [39].

The theoretical computations were performed density functional theory (DFT) method with Becke's 3-parameter exchange correlation-functional (B3) combined with correlation functional of Lee, Yang and Parr (LYP) (B3LYP) and B3 exchange correlation-functional combined with gradient-corrected correlation functional of Perdew and Wang's 1991 (B3PW91) method with 6-31+G(d,p) basis set in water solvent using CPCM model in build in Gaussian 09 Revision-A02 program package used for geometry optimization, IR wavenumbers ( $\text{cm}^{-1}$ ), global and local chemical properties and thermodynamic properties calculations. The elaborated vibrational assignments were performed on the idea of potential energy distributions (PED) analysis using VEDA 4 program [40] and visualized by using Gauss View 5.0 program. The theoretically calculated vibrational wavenumbers were scaled with 0.964 for B3LYP/6-31+G(d,p) and 0.960 scaling factor for B3PW91/6-31+G(d,p) level [41] and the calculated wavenumbers of 4B2AEAB molecule were correlate with experimental FT-IR spectrum. The proton and carbon-13 NMR chemical shifts of 4B2AEAB molecule were calculated using DFT/6-31+G(d,p) in the gas phase, water,  $\text{CHCl}_3$ , DMSO and DCM solvent in C-PCM model and the calculated chemical shifts showing good agreement with experimental  $^1\text{H}$  and  $^{13}\text{C}$  NMR chemical shifts in  $\text{CDCl}_3$  solvent and using gauge invariant atomic orbital

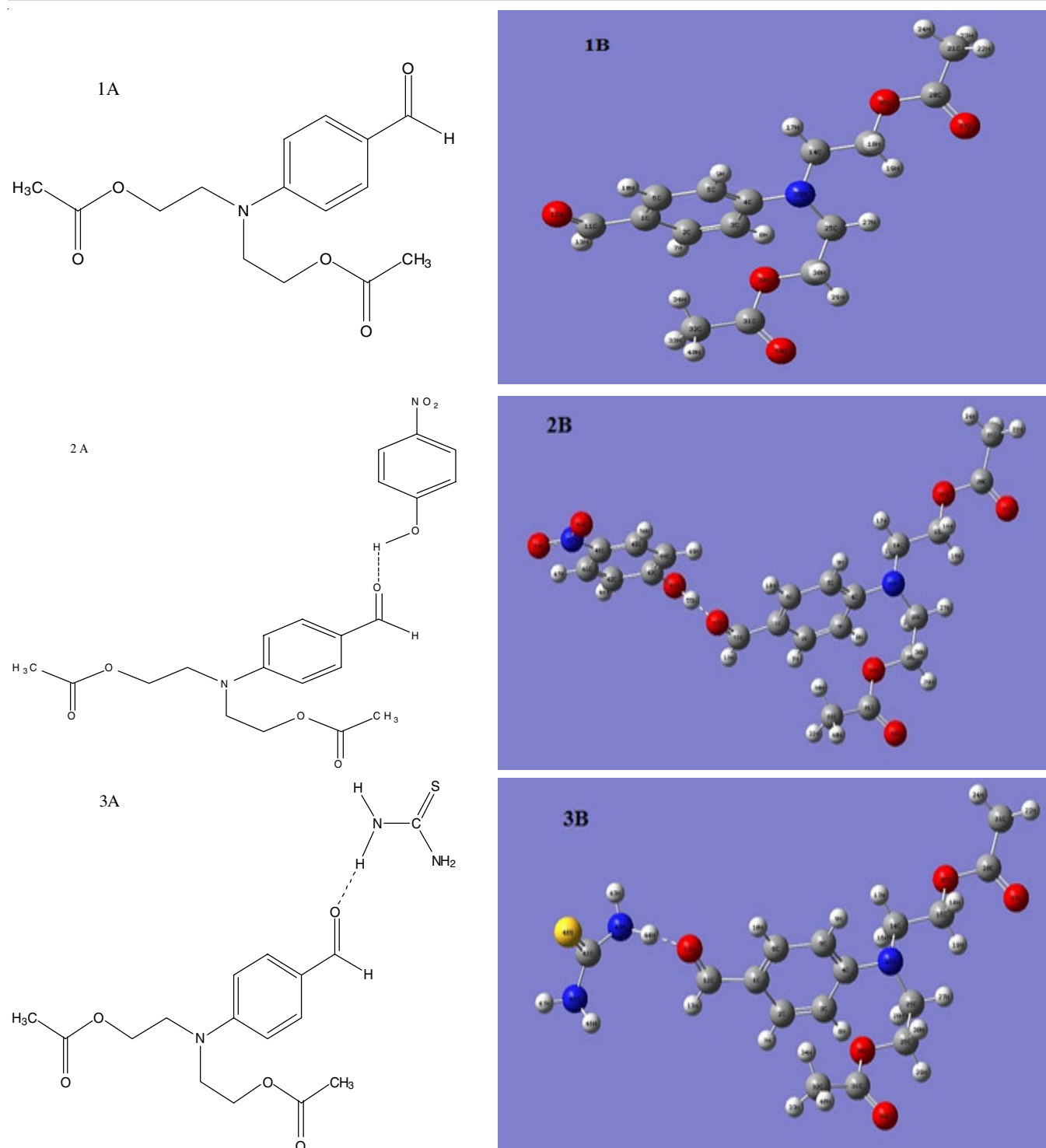


Fig. 1. Chemical structure and optimized molecular structure of 4B2AEAB (1A & 1B), 4B2AEAB4NP (2A & 2B) and 4B2AEABTU (3A & 3B), respectively

(GIAO method) approach [42,43]. The UV-visible absorption spectrum of 4B2AEAB and its derivatives computed were done using TD-DFT/6-31+G(d,p) method in the gas phase and in water, DMSO, CH<sub>2</sub>Cl<sub>2</sub> and CHCl<sub>3</sub> solvent using CPCM model and water solvent used for the derivatives. According to FMOs, the computed HOMO and LUMO energies values and their shapes of 4B2AEAB and its derivatives were simulated using DFT (B3LYP and B3PW91) using 6-31+G(d,p) basis set in

water solvent. The computed frontier molecular orbitals (FMOs) like HOMO and LUMO energy values of 4B2AEAB molecule, the various molecular (Global) properties such as electron affinity (A), ionization potential (I), chemical hardness ( $\eta$ ), chemical potential ( $\mu$ ), softness (S), electrophilicity index ( $\omega$ ) and  $Q_{\max}$  were computed. The calculation of local chemical reactivity descriptors such as Fukui function (FF) analyses using neutral, cationic and anionic charge densities (Mulliken

population analysis) of 4B2AEAB molecule were computed at DFT (B3LYP & B3PW91) with 6-31+G(d,p) level in water solvent. The non-linear optical (NLO) properties of 4B2AEAB, 4B2AEAB4NP and 4B2AEABTU molecules such as the mean polarizability ( $\alpha$ ), the anisotropy of the polarizability ( $\Delta\alpha$ ), first hyperpolarizability tensor ( $\beta$ ) and second hyperpolarizability tensor ( $\gamma$ ) were analyzed. The NBO analysis was done to understand the intermolecular charge transfer (ICT) or hyperconjugation interactions and interactions among bonds of 4B2AEAB molecule. The density of state (DOS), 2D-contour map plot and its 3D-MESP surface map was simulated using optimized geometry of 4B2AEAB molecule and its derivatives. The thermodynamic properties like thermal energy (E), heat capacity ( $C_v$ ) and entropy (S) *etc.* and the temperature effect on thermodynamic properties were computed using DFT/B3LYP/6-31+G(d,p) level in water solvent. Finally, *in silico* ADMET and biological properties analysis of 4B2AEAB molecule and its derivatives were done using free online server (Molinspiration, SwissADME and preADMET server).

## RESULTS AND DISCUSSION

**Geometry optimization and molecular structure:** The electronic structure of rationally designed novel non-linear optical materials such as 4-[*bis*[2-(acetyloxy)ethyl]amino]benzaldehyde (4B2AEAB) and hydrogen bonded adduct 4-[*bis*[2-(acetyloxy)ethyl]amino]benzaldehyde 4-nitro phenol (4B2AEAB4NP) and 4-[*bis*[2-(acetyloxy)ethyl]amino]benzaldehyde thiourea (4B2AEABTU) have been investigated, in order to assess the effect of addition of 4-nitrophenol and thiourea (it has both electron acceptor and electron withdrawing

groups) with organic molecule (4B2AEAB molecule) *via* H-bond for the enhancement of non-linear optical (NLO) response. The optimized molecular structure of 4B2AEAB molecule and its derivatives with the numbering scheme of the atoms are shown in the Fig. 1. The ground state energies and optimized geometric parameters of the 4B2AEAB molecule and its derivatives are given in the Table-1 and Table-2a-c, respectively. As seen in Table-2a-c, the calculated bond lengths of C2-C3 and C5-C6 are about 1.385 Å, 1.383 Å in B3LYP and 1.383 Å, 1.381 Å in B3PW91. The bond lengths C1-C2 and C3-C4 are largest about 1.408 Å, 1.422 Å in B3LYP and 1.405 Å, 1.419 Å in B3PW91 due to -CHO group attached from C1 carbon atom and amino group attached from C4 carbon atom. The bond lengths in C1-C11 and C4-N35 are about 1.456 Å, 1.381 Å in B3LYP and 1.454 Å, 1.375 Å in B3PW91. The hydrogen bond lengths O12-H55 in intermolecular H-bonded derivatives like 4B2AEAB4NP molecule are about 1.6333 Å and O12-H44 bond length in 4B2AEABTU molecule are about 2.001 Å in B3LYP level.

TABLE-1  
TOTAL ENERGY (a.u.), CHARGE AND MULTIPLICITY OF TITLE COMPOUND 4B2AEAB AND ITS DERIVATIVES USING DFT METHOD WITH 6-31+G (d, p) BASIS SET IN WATER SOLVENT

Compound	Charge/ Multiplicity	Total energy (a.u.)	
		B3LYP	B3PW91
4B2AEAB	Neutral/M=1	-1014.0141	-1013.6176
	Positive/M=2	-1013.6604	-1013.2594
	Negative/M=2	-1013.9811	-1013.5832
4B2AEAB4NP	Neutral/M=1	-1526.0458	-
4B2AEABTU	Neutral/M=1	-1562.2818	-

TABLE-2a  
SELECTED OPTIMIZED GEOMETRICAL DATA FOR 4-[*bis*[2-(ACETYLOXY)ETHYL]AMINO]BENZALDEHYDE (4B2AEAB) IN THE GROUND STATE CALCULATED AT DFT (B3LYP & B3PW91) METHOD IN WATER SOLVENT USING CPCM MODEL

Parameter	B3LYP	B3PW91	Parameter	B3LYP	B3PW91	Parameter	B3LYP	B3PW91	
Bond length	Å	Å	Bond length	Å	Å	Bond angle	(°)	(°)	
C1-C2	1.408	1.405	C20-O37	1.219	1.217	C4-N35-C25	122.10	122.08	
C1-C6	1.409	1.406	C21-H22	1.089	1.089	C14-N35-C25	116.35	116.35	
C1-C11	1.456	1.454	C21-H23	1.094	1.094	C15-C14-N35	112.52	112.28	
C2-C3	1.385	1.383	C21-H24	1.093	1.093	C26-C25-N35	115.48	115.33	
C2-H7	1.087	1.088	C25-C26	1.523	1.518	C15-O36-C20	177.13	116.67	
C3-C4	1.422	1.419	C25-H27	1.095	1.096	O36-C20-O37	122.87	122.84	
C3-H8	1.081	1.082	C25-H28	1.090	1.091	C21-C20-O36	111.54	111.51	
C4-C5	1.426	1.423	C25-N35	1.466	1.458	C21-C20-O37	125.57	125.63	
C4-N35	1.381	1.375	C26-H29	1.094	1.094	C26-O38-C31	117.05	116.48	
C5-C6	1.383	1.381	C26-H30	1.093	1.094	O38-C31-O39	122.94	122.92	
C5-H9	1.081	1.083	C26-O38	1.446	1.438	C32-C31-O38	111.60	111.54	
C6-H10	1.085	1.086	C31-C32	1.505	1.500	C32-C31-O39	125.45	125.52	
C11-O12	1.233	1.230	C31-O38	1.348	1.344	C4-N35-C14	121.04	121.00	
C11-H13	1.108	1.109	C31-O39	1.220	1.217	O12-C11-H13	119.45	119.59	
C14-C15	1.531	1.526	C32-H33	1.093	1.093	H16-C14-N35	108.01	107.97	
C14-H16	1.091	1.092	C32-H34	1.094	1.094	H17-C14-N35	110.86	111.03	
C14-H17	1.095	1.096	C32-H40	1.089	1.089	H27-C25-N35	108.09	108.25	
C14-N35	1.464	1.456	Bond angle (°)		Bond angle (°)		H28-C25-N35	109.69	109.65
C15-H18	1.092	1.093	C2-C1-C11	119.86	119.87	H18-C15-O36	109.23	109.39	
C15-H19	1.092	1.093	C6-C1-C11	122.36	122.26	H19-C15-O36	109.32	109.49	
C15-O36	1.446	1.437	C1-C11-O12	125.78	125.69	H29-C26-O38	109.23	109.41	
C20-C21	1.505	1.500	C3-C4-N35	121.79	121.72	H30-C26-O38	109.01	109.21	
C20-O36	1.349	1.345	C5-C4-N35	121.09	121.05	C31-C32-H40	109.73	109.76	

TABLE-2b  
SELECTED OPTIMIZED DIHEDRAL ANGLE (°) FOR 4-[bis[2-(ACETYLOXY)ETHYL]AMINO]BENZALDEHYDE (4B2AEAB) MOLECULE IN THE GROUND STATE CALCULATED AT DFT (B3LYP & B3PW91) METHOD IN WATER SOLVENT USING CPCM MODEL

Parameter	B3LYP	B3PW91	Parameter	B3LYP	B3PW91
Dihedral angle	(°)	(°)	Dihedral angle	(°)	(°)
C2-C1-C11-O12	179.637	179.6241	C14-C15-O36-C20	-179.4499	179.8634
C6-C1-C11-O12	0.1934	0.1657	O37-C20-O36-C15	-0.1721	-0.2086
C2-C1-C11-H13	-0.4398	-0.4612	O36-C20-C21-H22	177.4771	177.6342
C6-C1-C11-H13	-179.883	-179.9195	O37-C20-C21-H22	-2.703	-2.5613
C2-C3-C4-N35	-178.313	-178.2331	C25-C26-O38-C31	-178.8532	-178.4407
N35-C4-C5-C6	178.411	178.3093	O39-C31-O38-C26	-0.2908	-0.4231
C3-C4-N35-C25	12.9485	15.0031	C32-C31-O38-C26	179.5823	179.3918
C5-C4-N35-C25	-167.06	-165.0132	O38-C31-C32-H33	56.6071	55.6015
C5-C4-N35-C14	-175.473	6.1359	O39-C31-C32-H33	-123.5237	-124.5894
C26-C25-N35-C4	-105.246	-107.7857	O39-C31-C32-H34	118.2499	117.2065
C15-C14-N35-C4	78.5908	76.9941	O39-C31-C32-H40	-2.4043	-3.3607
N35-C4-C5-H9	-1.0503	-0.8628	O38-C31-C32-H34	-61.6193	-62.6026
H8-C3-C4-N35	3.6171	3.837	O38-C31-C32-H40	177.7264	176.8302
N35-C25-C26-O38	65.4858	65.4358	H16-C14-N35-C25	10.8681	8.8089
N35-C14-C15-O36	-177.877	-177.6723	H17-C14-N35-C25	127.1814	125.0533

TABLE-2c  
SELECTED BOND LENGTHS, BOND ANGLE AND DIHEDRAL ANGLE OF INTERMOLECULAR H-BONDED 4B2AEAB4NP AND 4B2AEABTU MOLECULE OPTIMIZED AT DFT/B3LYP/6-31+G (d, p) LEVEL IN WATER SOLVENT USING CPCM MODEL

Parameter's	4B2AEAB4NP	Parameter's	4B2AEABTU
Bond lengths	Å	Bond lengths	Å
O12-H55	1.6333	O12-H44	2.001
Bond angle	(°)	Bond angle	(°)
C11-O12-H55	121.0296	C11-O12-H44	137.9002
C43-O51-H55	112.5006	-	-
Dihedral angle	(°)	Dihedral Angle	(°)
C1-C11-O12-H55	179.0978	C1-C11-O12-H44	178.5408
H13-C11-O12-H55	-0.7716	H13-C11-O12-H44	-1.345
C42-C43-O51-H55	-180.0048	-	-
C44-C43-O51-H55	0.0349	-	-

The bond angles around C1 atom are C2-C1-C11=119.86° and 119.87°, C6-C1-C11= 122.36° and 122.26°, C1-C11-O12 = 125.78° and 125.69° at B3LYP and B3PW91 of 4B2AEAB, respectively and bond angle around C4 atom are C3-C4-N35 = 121.79° and 121.72°, C5-C4-N35 = 121.09° and 121.05°, C4-N35-C14 = 121.04° and 121.00°, C14-N35-C25 = 122.10° and 122.08°, C15-C14-N35 = 112.52° and 112.27°, C26-C25-N35 = 115.48° and 115.35° at B3LYP and B3PW91 of 4B2AEAB, respectively. The selected bond angles of 4B2AEAB4NP are C11-O12-H55 = 121.0296°, C43-O51-H55 = 112.5006° and bond angle of 4B2AEABTU are C11-O12-H44 = 137.9002° at B3LYP level. These asymmetries of bond angle reveals that the conjugation with the acetyloxy ethylamino side chain in 4B2AEAB molecule, conjugation with the 4-nitrophenol by hydrogen bond in 4B2AEAB4NP molecule and conjugation with the thiourea by hydrogen bond in 4B2AEABTU molecule take place resulting from the charge transfer interactions within the molecule and this type of properties increase the non-linear optical as well as biological property of the molecule. From Table 2b and 2c, the torsion angles of 4B2AEAB molecule are C2-C1-C11-O12 = 179.637° and 179.624°, C6-C1-C11-O12 = 0.1934° and 0.1657°, C2-C3-C4-N35 = -178.313° and -178.233°, N35-C4-C5-C6 = 178.411° and 178.309°, N35-

C14-C15-O36 = -177.877° and -177.672°, N35-C25-C26-O38 = 65.485° and 65.435° and O37-C20-O36-C15 = -0.1721° and -0.2086° in B3LYP and B3PW91 level. The selected dihedral angles of H-bonded 4B2AEAB4NP molecule are C1-C11-O12-H55 = 179.0978° and H13-C11-O12-H55 = -0.7716° and in H-bonded 4B2AEABTU molecule the dihedral angle are C1-C11-O12-H44 = 174.5408° and H13-C11-O12-H44 = -1.345° at B3LYP level shown in Table-2c. The above geometrical investigation of 4B2AEAB molecule and its derivatives shows that the variation in the bond lengths, bond angles and dihedral angles shows polymorphism this is most important property of organic compounds. Polymorphism is the most important factor for pharmaceutical industries [44], in the field of optoelectronic and photonics industries.

**Vibrational frequency analysis:** The molecule 4B2AEAB, 4B2AEAB4NP and 4B2AEABTU consist of 40, 55 and 48 atoms belongs to C<sub>1</sub> point group symmetry and has 114, 159 and 138 normal modes of fundamental vibrations, respectively. The comparative analysis of fundamental modes of vibrations with FT-IR (capillary cell technique = neat) wavenumbers and theoretically calculated wavenumbers (unscaled and scaled), IR intensities of 4B2AEAB using (B3LYP and B3PW91 levels) 4B2AEAB4NP (B3LYP) and 4B2AEABTU (B3LYP) with 6-

31+G (d,p) basis set in water solvent using CPCM model and visualized and assigned by GaussView 5.0.8 and VEDA 4 program are reported in Table-3a-c. The theoretically calculated wavenumbers are greater than experimental wavenumbers due to correlation effect of basis set and electrons inadequacy. For this reason, theoretically calculated wavenumbers were scaled with 0.9648 (for B3LYP/6-

31+G(d,p) level) and 0.9602 (for B3PW91/6-31+G(d,p) level) [41]. The spectra of the title molecule (4B2AEAB) and its H-bonded derivatives are shown in Fig. 2.

**C-H vibrations:** In aromatic and heterocyclic aromatic compounds, C-H stretching band appear in the range 3100-3000  $\text{cm}^{-1}$  and the C-H in-plane and out-of-plane bending vibrations are observed in the range of 1300-1000  $\text{cm}^{-1}$  and 900-675

TABLE-3a  
OBSERVED FT-IR AND CALCULATED WAVENUMBERS USING B3LYP AND B3PW91 WITH 6-31+G (d, p)  
BASIS SET FOR 4B2AEAB MOLECULE IN WATER SOLVENT USING CPCM MODEL

Mode	Experimental FT-IR ( $\text{cm}^{-1}$ )	B3LYP Wavenumber ( $\text{cm}^{-1}$ )		B3PW91 Wavenumber ( $\text{cm}^{-1}$ )		IR intensity	Assignments
		Unscaled	Scaled	Unscaled	Scaled		
1	3050	3248	3133	3251	3121	8.1783	$\nu_s(\text{C3-H8})$
2	-	3240	3125	3243	3113	15.715	$\nu_s(\text{C5-H9})$
3	-	3203	3090	3211	3083	4.56	$\nu_s(\text{C6-H10})$
4	-	3180	3068	3197	3069	16.033	$\nu_s(\text{C2-H7})$
5	-	3177	3065	3196	3068	9.6436	$\nu_s(\text{C21-H22})$
6	-	3176	3064	3190	3063	10.198	$\nu_s(\text{C32-H48})$
7	-	3143	3032	3155	3029	32.296	$\nu_s(\text{C25-H28})$
8	-	3141	3030	3154	3028	43.508	$\nu_s(\text{C14-H16})$
9	-	3133	3022	3153	3027	4.0325	$\nu_s(\text{C21-H23})$
10	-	3132	3021	3151	3025	3.9286	$\nu_s(\text{C32-H33})$
11	-	3124	3014	3133	3008	16.177	$\nu_s(\text{C26-H29})$
12	-	3119	3009	3130	3005	5.0755	$\nu_s(\text{C15-H19})$
13	-	3084	2975	3089	2966	34.941	$\nu_s(\text{C15-H})$
14	-	3075	2966	3081	2958	77.575	$\nu_s(\text{C26H})$
15	-	3066	2958	3077	2954	1.5966	$\nu_s(\text{C21-H3})$
16	-	3065	2957	3076	2953	0.7379	$\nu_s(\text{C32-H})$
17	2900	3063	2955	3069	2946	43.849	$\nu_s(\text{C25-H27})$
18	2810	3058	2950	3063	2941	38.992	$\nu_s(\text{C14-H17})$
19	2740	2991	2885	2993	2873	198.313	$\nu_s(\text{C11-H13})$
20	1740	1753	1691	1777	1706	562.802	$\nu_s(\text{C11-O12})$
21	1680	1752	1690	1774	1703	506.949	$\nu_s(\text{C28-O37})$
22	1600	1701	1641	1722	1653	416.851	$\nu_s(\text{C31-O39})$
23	1550	1631	1573	1645	1579	1528.735	$\nu_s(\text{C2-C3})$
24	1530	1582	1526	1596	1532	199.748	$\nu_s(\text{C5-C6})$
25	-	1554	1499	1562	1499	284.543	$\nu_s(\text{C4-C6})$
26	1450	1523	1469	1515	1454	26.876	$\nu_s(\text{C14-C15})$
27	1440	1512	1458	1505	1445	11.497	$\nu_{as}(\text{C14-C15})$
28	-	1500	1447	1495	1435	17.615	$\nu_s(\text{C25-C26})$
29	-	1499	1446	1494	1434	7.670	$\nu_{as}(\text{C25-C26})$
30	-	1475	1423	1478	1419	68.396	$\nu_{as}(\text{C2-C3})$
31	-	1467	1415	1461	1402	14.818	$\beta(\text{C21-H})$
32	-	1466	1414	1460	1401	15.254	$\beta(\text{C32-H})$
33	1390	1461	1409	1455	1397	30.339	$\beta(\text{C21-H})$
34	-	1461	1409	1454	1396	27.966	$\beta(\text{C32-H})$
35	-	1440	1389	1442	1384	74.417	$\beta(\text{C14-H})$
36	-	1431	1380	1432	1375	13.662	$\gamma(\text{C11-H})$
37	-	1422	1371	1425	1368	155.757	$\beta(\text{C14-H})$
38	-	1414	1364	1414	1357	226.735	$\beta(\text{C15-H})$
39	-	1402	1352	1399	1343	151.192	$\nu_s(\text{C25-H})$
40	-	1398	1348	1395	1339	33.133	$\beta(\text{C21-H}), \gamma(\text{CCN})$
41	1330	1391	1342	1386	1330	89.754	$\beta(\text{C32-H}), \gamma(\text{CCH})$
42	1320	1371	1322	1383	1327	10.610	$\beta(\text{C4-N35}), \gamma(\text{CCC})$
43	-	1347	1299	1346	1273	170.76	$\beta(\text{C14-H}), \gamma(\text{OHC})$
44	-	1342	1294	1334	1280	16.546	$\beta(\text{C5-C6}), \gamma(\text{COH})$
45	-	1318	1271	1319	1266	15.748	$\beta(\text{C14-C15}), \gamma(\text{CCC})$
46	1230	1301	1255	1302	1250	77.179	$\beta(\text{C25-C26}), \gamma(\text{CCH})$
47	-	1274	1229	1276	1225	24.949	$\beta(\text{C1-C11}), \gamma(\text{CCH})$
48	-	1268	1223	1273	1222	227.833	$\gamma(\text{C31-O38}), \gamma(\text{OOH})$
49	-	1261	1216	1272	1221	563.970	$\gamma(\text{C31-O38}), \gamma(\text{NCH})$
50	-	1260	1215	1266	1215	657.209	$\gamma(\text{C28-O36}), \gamma(\text{OCH})$
51	1170	1248	1204	1250	1200	151.576	$\gamma(\text{C14-C15}), \gamma(\text{HCH})$

52	-	1203	1160	1210	1161	80.274	$\beta$ (C14-N35), $\gamma$ (CCH)
53	1130	1190	1148	1190	1142	619.794	$\beta$ rock(C1-C11), $\gamma$ (CCH)
54	-	1154	1113	1152	1106	1.0825	$\beta$ rock(C2-C3), $\gamma$ COH
55	-	1143	1102	1143	1097	159.381	$\beta$ scisC14-N-C25), $\gamma$ HCH
56	1050	1102	1063	1108	1063	26.708	rock(C14-N-C25), $\gamma$ HCC
57	-	1081	1042	1094	1050	17.951	$\gamma$ (C14-C15-O36), $\gamma$ HCC
58	-	1064	1026	1077	1034	117.167	$\beta$ (C26-O38-C31), $\gamma$ HCC
59	-	1063	1025	1075	1032	12.853	$\gamma$ (O38-C31-C32), $\gamma$ HCO
60	1000	1062	1024	1057	1014	44.617	$\beta$ (O36-C20-C21) $\gamma$ HCC
61	990	1060	1022	1056	1013	191.617	$\gamma$ (C15-O36), $\gamma$ OHC
62	-	1028	991	1031	989	4.893	$\gamma$ (HCH)
63	-	1025	988	1028	987	35.587	$\gamma$ (HCO)
64	-	1012	976	1011	970	5.156	$\gamma$ (CCC)
65	-	1003	967	1004	964	27.211	$\gamma$ (HOC)
66	-	986	951	990	950	1.1112	$\gamma$ (OCC)
67	-	982	947	985	945	5.8964	$\gamma$ (HCH)
68	-	965	931	971	932	4.5515	$\gamma$ (HCH)
69	910	961	927	963	924	76.625	$\gamma$ (CCH)
70	-	916	883	926	889	4.1039	$\gamma$ (HCH)
71	830	910	877	920	883	34.989	$\gamma$ (HCH)
72	-	850	820	853	819	26.329	$\gamma$ (HNH)
73	-	832	802	837	803	13.283	$\gamma$ (CHC)
74	-	827	797	825	792	96.425	$\gamma$ (HOH)
75	740	814	785	813	780	13.597	$\tau$ HCHC
76	710	796	767	790	758	5.2874	$\tau$ OHCC
77	-	735	709	740	710	48.341	$\tau$ HCHC
78	640	723	697	722	693	4.4138	$\tau$ HCHC
79	-	649	626	649	623	16.267	$\tau$ HCHC
80	-	643	620	648	622	7.1764	$\tau$ HNHC
81	-	635	612	640	614	7.8024	$\tau$ HOHC
82	600	621	599	620	595	45.492	$\tau$ COHC
83	-	606	584	608	583	10.314	$\tau$ HCHC
84	-	605	583	607	582	10.193	$\tau$ HNHC
85	510	539	520	539	517	7.7557	$\tau$ COHC
86	-	526	507	525	504	4.8789	$\tau$ HCHC
87	-	504	486	502	482	2.1037	$\tau$ HNHC
88	-	487	469	484	464	30.8002	$\tau$ HOCC
89	-	439	423	440	422	17.050	$\tau$ HCHC
90	-	434	418	432	414	11.339	$\tau$ HCCC
91	-	414	399	414	397	14.490	$\tau$ HCOC
92	-	360	347	361	346	9.3294	$\tau$ HCCC
93	-	356	343	355	340	18.879	$\tau$ CCHC
94	-	316	304	315	302	1.8360	$\tau$ HCHC
95	-	303	292	299	287	2.3644	$\tau$ HCCC
96	-	265	255	267	256	2.0876	$\tau$ CCHC
97	-	255	245	253	242	24.771	$\tau$ OCCC
98	-	204	196	204	195	2.662	$\tau$ NCHC
99	-	198	191	198	190	3.374	$\tau$ CHCO
100	-	178	171	177	169	14.535	$\tau$ HCHC
101	-	174	167	173	166	9.665	$\tau$ HCHO
102	-	155	149	155	148	12.826	$\tau$ CCHC
103	-	124	119	124	119	3.2822	$\tau$ HCHC
104	-	110	106	109	104	0.7875	$\tau$ HCHC
105	-	89	85	90	86	2.596	$\tau$ CCHC
106	-	66	63	64	61	2.0803	$\tau$ CCHO
107	-	53	51	48	46	0.0909	$\tau$ COCH
108	-	50	48	42	40	0.1564	$\gamma$ COCH
109	-	45	43	41	39	2.9718	$\gamma$ CCCC
110	-	32	30	29	27	5.2619	$\gamma$ CCCH
111	-	26	25	25	24	2.1005	$\gamma$ COCC
112	-	23	22	20	19	4.6177	$\gamma$ CCCC
113	-	16	15	16	15	3.7640	$\gamma$ CCCC
114	-	15	14	14	13	0.0379	$\gamma$ CCOC

v = stretching; s = symmetric; as = asymmetric; scis = scissoring; rock = rocking;  $\beta$  = in-plane bending;  $\gamma$  = out-of-plane bending;  $\tau$  = torsion.

TABLE-3b  
THE CALCULATED WAVENUMBERS USING B3LYP WITH 6-31+G (d, p) BASIS SET  
FOR 4B2AEAB4NP MOLECULE IN WATER SOLVENT USING CPCM MODEL

Mode	<sup>2</sup> Scaled $\nu$ (cm <sup>-1</sup> )	IR intensity	Assignments	Mode	<sup>2</sup> Scaled $\nu$ (cm <sup>-1</sup> )	IR intensity	Assignments
159	3135	5.1343	$\nu_s$ (C3-H8)	126	1470	23.725	$\beta$ CH2et, $\nu_s$ (CH)R1
158	3129	3.8908	$\nu_s$ (C41-H47)	125	1468	527.172	$\nu_s$ N-O, $\beta$ (CCC)R2
157	3128	1.6937	$\nu_s$ (C45-H50)	124	1457	13.673	$\beta$ (CH2)ester
156	3127	11.2638	$\nu_s$ (C5-H9)	123	1449	57.1943	$\beta$ (CH2)ester
155	3103	1.2705	$\nu_s$ (C44-H49)	122	1445	4.0896	$\beta$ (CH2)
154	3102	7.4461	$\nu_s$ (C42-H48)	121	1433	236.202	$\beta$ CCO, $\nu_s$ NO
153	3034	3.2994	$\nu_s$ (C6-H10)	120	1427	173.482	$\beta$ CH2, $\gamma$ CCC
152	3074	16.434	$\nu_s$ (C2-H7)	119	1416	16.725	$\gamma$ CH3meth
151	3066	9.5909	$\nu_s$ (C21-H22)	118	1415	14.941	$\gamma$ CH3
150	3065	9.7724	$\nu_s$ (C32H)	117	1409	26.844	$\gamma$ CH3
149	3038	23.555	$\nu_s$ (C25H)	116	1409	30.537	$\gamma$ CH3
148	3031	44.977	$\nu_s$ (C15H)eth	115	1394	61.303	$\gamma$ CH2, $\gamma$ CNC
147	3023	4.2892	$\nu_s$ (C32H)meth	114	1390	117.354	$\gamma$ CCO, $\nu_{as}$ (CC)R1
146	3022	3.8251	$\nu_s$ (C21H)eth	113	1381	50.423	$\gamma$ CHOald, $\gamma$ CH2
145	3016	17.9052	$\nu_s$ (C26H)eth	112	1373	359.580	$\gamma$ CCN, $\nu_s$ CN
144	3013	2.3881	$\nu_s$ (C14H)eth	111	1365	181.274	$\beta$ CH2
143	2974	37.346	$\nu_s$ (C15H)eth	110	1352	130.062	$\beta$ CH3, $\beta$ CH2
142	2969	424.551	$\nu_s$ (C25H)eth	109	1349	38.810	$\beta$ CH3
141	2966	4777.85	$\nu_s$ (O51-H55)	108	1342	136.103	$\beta$ CH2, $\beta$ CH3
140	2960	262.331	$\nu_s$ (O51-H55)	107	1327	14.915	$\beta$ CCN, $\beta$ CH2
139	2958	66.288	$\nu_s$ (C14H)eth	106	1305	42.894	$\beta$ CCOp, $\beta$ CH2
138	2957	1.4169	$\nu_s$ (C32H)meth	105	1302	261.191	$\beta$ CH2, $\beta$ CCC
137	2957	0.3595	$\nu_s$ (C21H)meth	104	1299	47.279	$\nu_s$ CC, $\beta$ CH2
136	2889	375.20	$\nu_s$ (C11H) $\nu_s$ (OH)ph	103	1298	312.550	$\nu_s$ (CC)R2, $\nu_s$ NO2
135	1692	551.63	$\nu_s$ (C20-O37)ester	102	1274	14.538	$\nu_{as}$ (CC)R2, $\beta$ CCC
134	1690	515.65	$\nu_s$ (C31O39)ester	101	1264	1613.125	$\nu_{as}$ CC, $\nu_s$ CO,
133	1617	129.44	$\nu_s$ (C11O12)ald	100	1255	96.655	$\beta$ CH2
132	1587	180.80	$\beta$ CCC, $\nu_s$ OH	99	1242	506.894	$\beta$ CCO, $\beta$ CCC
131	1573	493.78	$\beta$ CCOp, $\nu_s$ CH	98	1236	319.193	$\nu_s$ CC, $\beta$ (CCH)R2
130	1559	1974.37	$\beta$ CCC, $\nu_s$ CO ald	97	1224	99.1846	$\nu_{as}$ CH2, $\nu_{as}$ CC
129	1517	266.74	$\beta$ CCCR1, $\nu_s$ (CH)R2	96	1216	725.222	$\gamma$ CCH, $\nu_s$ (C-O)ester
128	1500	634.01	$\beta$ CNCR1, $\nu_s$ CNR2	95	1215	514.783	$\beta$ COC, $\beta$ CCH
127	1491	177.61	$\nu_s$ NO, $\nu_s$ (OH)R1	94	1206	220.094	$\nu_{as}$ CC

$\nu$  = stretching;  $s$  = symmetric;  $as$  = asymmetric;  $scis$  = scissoring;  $rock$  = rocking;  $\beta$  = in-plane bending;  $\gamma$  = out-of-plane bending;  $\tau$  = torsion; R1 = benzaldehyde ring, R2 = phenol ring; eth = ethyl; meth = methyl; ald = aldehyde

TABLE-3c  
CALCULATED WAVENUMBERS USING B3LYP WITH 6-31+G (d, p) BASIS SET FOR  
4B2AEABTU MOLECULE IN WATER SOLVENT USING CPCM MODEL

Mode	<sup>3</sup> Scaled $\nu$ (cm <sup>-1</sup> )	IR intensity	Assignments	Mode	<sup>3</sup> Scaled $\nu$ (cm <sup>-1</sup> )	IR intensity	Assignments
138	3585	200.351	$\nu_s$ N45H	104	1446	3.0262	$\beta$ C26H
137	3579	216.938	$\nu_s$ N42H	103	1426	108.266	$\nu_s$ CC, $\beta$ C14H
136	3387	879.275	$\nu_s$ N45H	102	1416	14.635	$\beta$ C32H
135	3340	551.670	$\nu_s$ N42H	101	1415	14.544	$\beta$ C21H
134	3135	7.1558	$\nu_s$ C3H	100	1415	173.617	$\nu_s$ C41N, $\nu_s$ NH2
133	3126	13.665	$\nu_s$ C5H	99	1409	30.556	$\beta$ C21H
132	3092	5.1450	$\nu_s$ C6H	98	1409	28.521	$\beta$ C32H
131	3072	13.8078	$\nu_s$ C2H	97	1392	97.102	$\beta$ C14H
130	3065	9.6714	$\nu_s$ (C21H)meth	96	1382	31.666	$\nu_s$ C11H
129	3065	10.1222	$\nu_s$ (C32H)meth	95	1370	212.68	$\beta$ C15H
128	3036	23.192	$\nu_s$ (C25H)eth	94	1364	123.92	$\beta$ C25H
127	3031	49.917	$\nu_s$ C14H, $\nu_s$ (C15H)eth	93	1357	965.46	$\nu_s$ C-NH2, $\beta$ NH2
126	3022	3.8403	$\nu_s$ C32Hmeth	92	1352	238.071	$\beta$ C32H, $\beta$ C25H
125	3022	3.8665	$\nu_s$ C21Hmeth	91	1349	39.682	$\beta$ C21H

124	3014	19.195	$\nu_s$ C26H	90	1341	151.14	$\beta$ C32H, $\beta$ C25H
123	3012	3.257	$\nu_s$ C14H, $\nu_s$ C15H	89	1325	17.943	$\nu_s$ CC, $\nu_s$ C4-N35
122	2974	40.051	$\nu_s$ C15H	88	1301	236.35	$\nu_s$ (CC)b, $\nu_s$ (CH)b
121	2966	87.986	$\nu_s$ C26H	87	1298	11.336	$\nu_s$ (CH), $\nu_s$ CC, rockCH2
120	2958	40.672	$\nu_s$ C14H	86	1271	14.005	$\beta$ C14H
119	2957	9.947	$\nu_s$ (C32H)meth	85	1255	81.294	$\beta$ C25H
118	2957	0.9327	$\nu_s$ C21H	84	1233	98.428	$\nu_s$ C11H, $\nu_{as}$ CC, $\nu_s$ CH
117	2956	17.300	$\nu_s$ C14H	83	1221	89.159	$\beta$ C26H
116	2878	153.094	$\nu_s$ (C11H)ald	82	1216	744.18	$\nu_s$ C31-O
115	1692	557.39	$\nu_s$ (C20=O)ester	81	1214	539.015	$\nu_s$ C20-O
114	1690	509.80	$\nu_s$ (C31=O)ester	80	1205	173.508	$\beta$ C15H, $\beta$ CC
113	1629	405.91	$\nu_s$ (C11=O), $\nu_s$ NH2	79	1159	177.678	$\beta$ CHb, $\beta$ CH2
112	1595	188.84	$\nu_s$ NH2	78	1151	665.29	$\beta$ (CH)R1, $\beta$ CC
111	1567	469.41	$\nu_s$ NH2	77	1115	1.4711	$\beta$ CH, $\nu_s$ CC
110	1562	1692.3	$\nu_s$ NH2, $\nu_s$ CC	76	1101	152.37	$\beta$ CH2rock
109	1520	299.08	$\nu_s$ CC	75	1060	26.025	$\beta$ CH2rock
108	1501	438.78	$\nu_s$ CC	74	1053	47.065	$\beta$ NH2rock
107	1469	35.115	$\beta$ C14H	73	1046	24.282	$\beta$ NH2rock
106	1456	13.290	$\beta$ C15H	72	1043	20.864	$\nu_s$ C14-C15
105	1448	34.869	$\beta$ C25H	52	712	30.1045	$\nu_s$ C41-S48, $\gamma$ NH2

$\nu$  = stretching;  $s$  = symmetric;  $as$  = asymmetric;  $scis$  = scissoring; rock = rocking;  $\beta$  = in-plane bending;  $\gamma$  = out-of-plane bending;  $\tau$  = torsion; R1 = benzaldehyde; ald = aldehyde; b = benzene

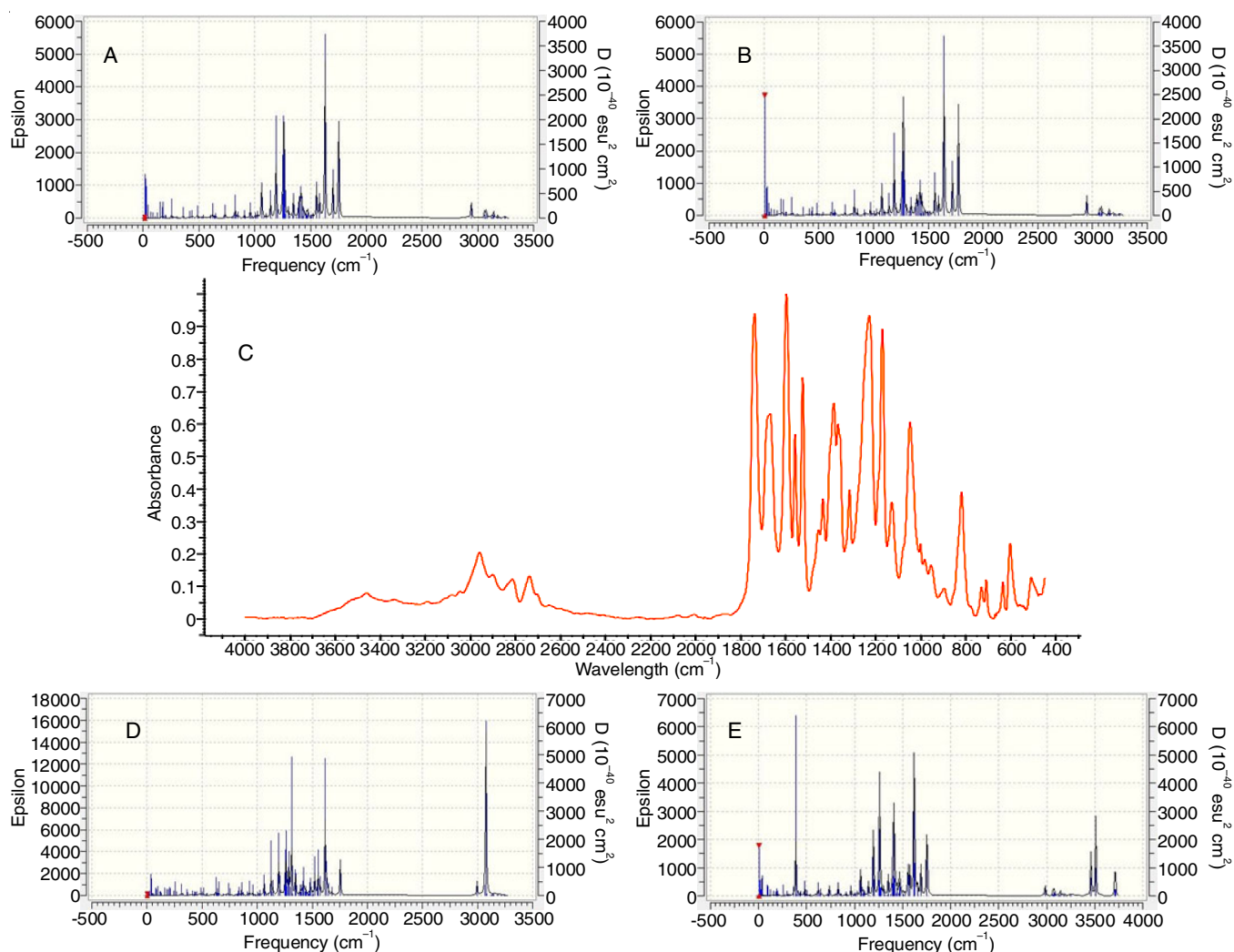


Fig. 2. IR-spectrum plot A and B of 4B2AEAB at B3LYP and B3PW91, plot C FT-IR spectrum of 4B2AEAB at  $CDCl_3$  [37], plot D of 4B2AEAB4NP at B3LYP and plot E of 4B2AEABTU at B3LYP level in water solvent

$\text{cm}^{-1}$  given in the literature [45], respectively. The calculated IR wavenumbers were observed in the range of 3133-3068  $\text{cm}^{-1}$  and 3121-3069  $\text{cm}^{-1}$  at B3LYP and B3PW91 level, respectively and the C-H stretching vibrations which correlated well with the experimental FT-IR band was observed at 3050  $\text{cm}^{-1}$ . The C-H stretching vibrations in  $sp^3$  hybridized molecule were appearing in the range of 3000-2800  $\text{cm}^{-1}$  [45]. In present study, the calculated C-H stretching bands appear in the range of 3065-2885 and 3068-2873  $\text{cm}^{-1}$  at B3LYP and B3PW91 level, respectively and correlated with experimental FT-IR bands observed in the range of 2900-2740  $\text{cm}^{-1}$ . The calculated C-H in-plane bending and out-of-plane vibrations at B3LYP and B3PW91 were observed at 1322 & 1327  $\text{cm}^{-1}$  and 991 & 981  $\text{cm}^{-1}$ , respectively, which correlated well with the experimental FT-IR band observed at 1320  $\text{cm}^{-1}$  of in-plane vibrations and 910  $\text{cm}^{-1}$  of out-of plane vibrations. The C-H stretching vibration of aldehyde with strong intensity appear in two bands in region 2850-2820 and 2750-2720  $\text{cm}^{-1}$  [45] and in the present study, the calculated C-H stretching vibration observed in region 2885-2873  $\text{cm}^{-1}$  with strong intensity in B3LYP and B3PW91 level, respectively and correlated well with experimental FT-IR bands observed in region 2740  $\text{cm}^{-1}$ .

**C=O and C-O vibrations:** The band due to C=O stretching vibration of aromatic aldehyde were observed in the region 1740-1720  $\text{cm}^{-1}$  and C=O of ester appear in region 1750-1700  $\text{cm}^{-1}$  [45]. In present study, the calculated C=O stretching vibration of aromatic aldehyde and ester side chain of 4B2AEAB were observed at B3LYP and B3PW91 1691  $\text{cm}^{-1}$  and 1690-1641  $\text{cm}^{-1}$  and 1706  $\text{cm}^{-1}$  and 1703-1653  $\text{cm}^{-1}$ , respectively and correlate well with experimental FT-IR bands observed in region 1740  $\text{cm}^{-1}$  and 1680-1600  $\text{cm}^{-1}$  of aromatic aldehyde and ester side chain, respectively.

**C-C and C-N vibrations:** The ring C-C stretching vibrations lie in the region 1600-1400  $\text{cm}^{-1}$  with medium, weak and variable intensity [45] and according to Versanyi [46], the five bands lie in the region 1625-1590, 1590-1575, 1540-1470, 1465-1430 and 1380-1280  $\text{cm}^{-1}$ . In present study, the calculated five C-C stretching vibrations of 4B2AEAB at B3LYP and B3PW91 were found in the region 1573-1526, 1469-1423, 1294-1223, 1204, 1148-1113  $\text{cm}^{-1}$  and 1579-1532, 1454-1419, 1280-1225, 1200, 1142-1106, respectively and all five bands show good agreement with experimental FT-IR band lie in range 1550-1530, 1450-1440, 1230, 1170, 1130  $\text{cm}^{-1}$ . According to Sundaraganesan *et al.* [47] assigned the C-N stretching vibrations at 1302  $\text{cm}^{-1}$  and Kumar and Ramasamy [48] have assigned C-N stretching band at 1256  $\text{cm}^{-1}$ . The calculated C-N stretching band assigned at B3LYP and B3PW91 level in region 1322, 1160, 1327 and 1161  $\text{cm}^{-1}$ , respectively and the observed peak agreed well with the experimental FT-IR values at 1320  $\text{cm}^{-1}$ . The C-N stretching vibrations of 4B2AEAB4NP and 4B2AEABTU compounds appear in the region 1373 and 1415  $\text{cm}^{-1}$ , respectively (Table-3b and 3c).

**N-H and C-S vibrations:** In the all heterocyclic organic compounds the N-H stretching vibrations found in the region 3500-3300  $\text{cm}^{-1}$  [49]. From literature survey, Sathiya *et al.* [31] showed the N-H stretching vibrations in the region 3370  $\text{cm}^{-1}$  and 3391  $\text{cm}^{-1}$  in experimental FT-IR. In this work, the

N-H stretching vibrations occur in the region 3585-3540  $\text{cm}^{-1}$  in theoretically calculated wavenumbers of 4B2AEABTU compound at B3LYP/6-31+G(d,p) basis set in water solvent reported in Table-3c. The C-S stretching vibrations appear in the range of 930-670  $\text{cm}^{-1}$  was given in literature [50]. The FT-IR bands appear in the region 728  $\text{cm}^{-1}$  [31] and the calculated C-S stretching vibrations of 4B2AEABTU appear in the region 712  $\text{cm}^{-1}$  at B3LYP/6-31+G(d,p) basis set in water solvent given in Table-3c. The above values of literature and experimental FT-IR matched well with the theoretical wavenumbers.

**N-O and O-H vibrations:** The N-O stretching bands appear in 1585-1498  $\text{cm}^{-1}$  region [32], while the N-O stretching vibrations of intermolecular hydrogen bonded 4B2AEAB4NP calculated at B3LYP/6-31+G(d,p) basis set in water solvent occur in the region 1491, 1468, 1433  $\text{cm}^{-1}$  and symmetrical stretching vibration found in the region 1298  $\text{cm}^{-1}$  due to  $-\text{NO}_2$  group of phenol match well with FT-IR bands [32] appeared at 1370  $\text{cm}^{-1}$  due to symmetrical stretching mode of  $-\text{NO}_2$  group of phenol. The O-H stretching vibrations appeared at 3086  $\text{cm}^{-1}$  [32] and in the present study, the O-H stretching bands assigned in the region 2966-2960, 2889 and 1587  $\text{cm}^{-1}$  due to the intermolecular hydrogen bonding where the -OH stretching bands is expected to shift towards lower frequency calculated at B3LYP level and matched well with experimental FT-IR bands.

**NMR spectral analysis:** Nuclear magnetic resonance (NMR) is the powerful technique for conformational analysis of organic and inorganic compounds [51,52]. The optimized structure of title molecule (4B2AEAB) was affirmed by  $^1\text{H}$  and  $^{13}\text{C}$  NMR chemical shifts by employing DFT/B3LYP/6-31+G(d,p) basis set in the gas phase and solvents ( $\text{CHCl}_3$ , water, DMSO and  $\text{CH}_2\text{Cl}_2$ ) using CPCM model and compared with experimental [37]  $^1\text{H}$  &  $^{13}\text{C}$  chemical shifts (in  $\text{CDCl}_3$ ). The theoretical and experimental  $^1\text{H}$  and  $^{13}\text{C}$  NMR chemical shifts values are summarized in Table-4. The observed  $^1\text{H}$  NMR spectrum of 4B2AEAB shows the presence of one distinct singlet appeared at  $\delta$  2.04 ppm of  $-\text{OOC}-(\text{CH}_3)$  methyl proton of 4-[bis[2-(acetyloxy)ethyl]-amino]benzaldehyde (4B2AEAB) and the theoretical chemical shift values of protons of methyl group for H22, H23, H24 and H33, H34, H40 atoms in  $\text{CHCl}_3$ , gas phase, water, DMSO and  $\text{CH}_2\text{Cl}_2$  solvents appeared at 1.72-2.12 ppm, 1.56-2.01 ppm, 1.77-2.03 ppm, 1.78-2.10 ppm and 1.74-2.09 ppm and 1.46-1.56 ppm, 1.28-1.54 ppm, 1.51-1.57 ppm, 1.52-1.58 ppm and 1.49-1.56 ppm, respectively and other singlet appeared in deshielded at  $\delta$  9.71 ppm is to CH proton of carbonyl group of 4B2AEAB and calculated chemical shift of C-H13 proton in  $\text{CHCl}_3$ , gas phase, water, DMSO and  $\text{CH}_2\text{Cl}_2$  solvent appeared at 9.71 ppm, 10.40 ppm, 10.43 ppm, 10.39 ppm, 10.396 ppm and 10.40 ppm, respectively. In the aromatic ring, four doublets correspond to protons of aromatic  $-\text{CH}$  group of 4B2AEAB ring. The simulated  $^1\text{H}$  NMR spectrum of 4B2AEAB compound is shown in Fig. 3a.

Further,  $^{13}\text{C}$  NMR spectrum exhibits the distinct signals at  $\delta$  190.27 ppm,  $\delta$  170.84 ppm and  $\delta$  20.76 ppm for C=O group of aldehyde, two acetyloxy groups and two  $-\text{CH}_3$  groups of 4B2AEAB, respectively. The calculated chemical shift of C=O of aldehyde of 4B2AEAB in  $\text{CHCl}_3$ , gas phase, water, DMSO and DCM solvents appeared at 189.53 ppm, 186.22

TABLE-4a  
OBSERVED (in CDCl<sub>3</sub>) AND CALCULATED <sup>1</sup>H NMR USING DFT/B3LYP/6-31+G (d, p)  
BASIS SET IN THE GAS PHASE AND SOLVENT PHASE FOR 4B2AEB MOLECULE

Nucleus	CDCl <sub>3</sub>	CHCl <sub>3</sub>	Gas	Water	DMSO	DCM	Assignments
	$\delta_{exp}^*$	$\delta_{cal}$	$\delta_{cal}$	$\delta_{cal}$	$\delta_{cal}$	$\delta_{cal}$	
7H	6.79	7.50	7.29	7.57	7.56	7.53	d, 1H, CH- phenyl ring, 'o' position
8H	7.71	8.91	8.75	8.96	8.95	8.93	d, 1H, CH -phenyl ring, 'm' position
9H	6.79	7.40	7.32	7.42	7.43	7.41	d, 1H, CH- phenyl ring, 'm' position
10H	7.71	8.619	8.612	8.60	8.61	8.62	d, 1H, CH- phenyl ring, 'o' position
13H	9.71	10.40	10.43	10.39	10.396	10.40	s, 1H, CH-(CHO group, aldehyde)
16H	3.70	2.31	2.54	2.34	2.35	2.32	t, 4H, CH <sub>2</sub> - methylene
17H	3.70	2.80	2.77	2.81	2.82	2.80	
18H	4.29	3.36	3.27	3.37	3.38	3.36	
19H	4.29	5.07	5.05	5.07	5.08	5.07	
22H	2.04	2.12	2.01	2.09	2.10	2.09	t, 4H, CH <sub>2</sub> - methylene
23H	2.04	2.12	1.98	2.17	2.18	2.15	
24H	2.04	1.72	1.56	1.77	1.78	1.74	
27H	3.70	2.95	2.87	2.97	2.98	2.96	
28H	3.70	3.36	3.20	3.41	3.42	3.39	s, 6H, CH <sub>3</sub> (methyl group)
29H	4.29	4.60	4.61	4.59	4.60	4.6	
30H	4.29	3.07	3.01	3.05	3.06	3.054	
33H	2.04	1.46	1.28	1.51	1.52	1.49	
34H	2.04	0.60	0.56	0.62	0.63	0.61	
40H	2.04	1.56	1.51	1.57	1.58	1.56	

TABLE-4b  
OBSERVED (in CDCl<sub>3</sub>) AND CALCULATED <sup>13</sup>C NMR USING DFT/B3LYP/6-31+G (d, p)  
BASIS SET IN THE GAS PHASE AND SOLVENT PHASE FOR 4B2AEB MOLECULE

Nucleus	CDCl <sub>3</sub>	CHCl <sub>3</sub>	Gas	Water	DMSO	DCM	Assignments
	$\delta_{exp}^*$	$\delta_{cal}$	$\delta_{cal}$	$\delta_{cal}$	$\delta_{cal}$	$\delta_{cal}$	
1C	126.09	131.85	131.58	131.96	131.97	131.91	Phenyl ring
2C	111.36	112.19	111.31	112.52	112.51	112.35	
3C	132.18	125.65	124.94	125.935	125.92	125.79	
4C	152.30	155.23	154.12	155.61	155.59	155.42	
5C	111.36	110.84	110.98	110.76	110.77	110.81	
6C	132.18	121.05	121.00	120.97	120.98	121.02	
11C	190.27	189.53	186.22	190.54	190.50	190.03	-CHO group
14C	49.56	46.99	47.58	46.81	46.42	46.90	Methylene group
15C	61.00	54.93	55.05	54.91	54.92	54.93	
20C	170.84	183.6	180.75	184.45	184.42	184.02	Carbonyl group
21C	20.76	12.51	11.71	12.76	12.75	12.63	Methyl group
25C	49.56	37.89	38.14	37.823	37.826	37.85	Methylene group
26C	61.00	54.91	54.65	54.997	54.99	54.95	
31C	170.84	183.29	180.34	184.18	184.14	183.72	Carbonyl group
32C	20.76	12.09	11.43	12.30	12.29	12.19	Methyl group

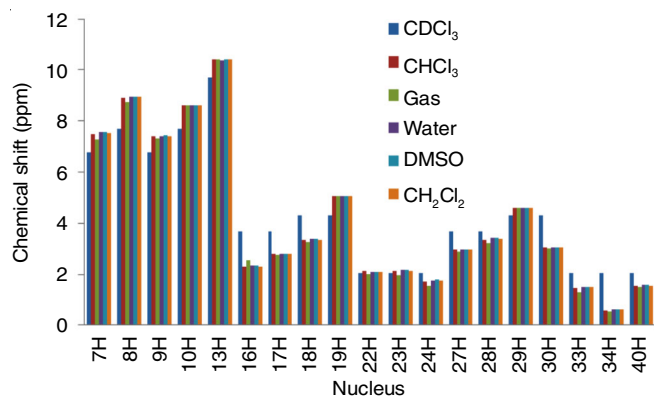


Fig. 3a. Simulated and correlated <sup>1</sup>H NMR spectrum of the title molecule 4B2AEB at experimental in CDCl<sub>3</sub> [37] and DFT/B3LYP/6-31+G(d,p) in gas phase and different solvent using CPCM model

ppm, 190.54 ppm 190.50 ppm and 190.03 ppm, respectively and the calculated chemical shift of C=O of acetyloxy in CHCl<sub>3</sub>, gas phase, water, DMSO and CH<sub>2</sub>Cl<sub>2</sub> solvents groups appeared at 183.29-183.6 ppm, 180.34-180.75 ppm, 184.18-184.45 ppm, 184.14-184.42 ppm and 183.72-184.02 ppm, respectively. From Table-4b, it is clear that the calculated chemical shift shows good agreement with experimental <sup>13</sup>C NMR chemical shift (in CDCl<sub>3</sub>). The simulated <sup>13</sup>C NMR spectrum of 4B2AEB compound is shown in Fig. 3b.

**UV-visible analysis:** The time dependent-density functional theory (TD-DFT) computational methods are well known and broadly engaged in the calculation of electronic spectra of compounds. In present study, one electron excitations between the molecular orbitals are generally explains the transition from ground state to excited state. This analysis provides excited state

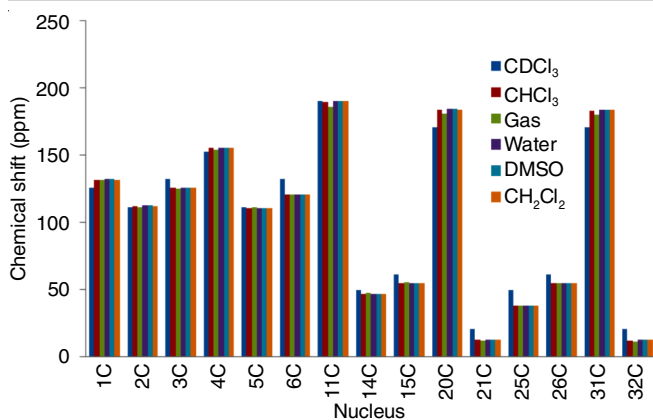


Fig. 3b. Simulated and correlated  $^{13}\text{C}$  NMR spectrum of 4B2AEAB compound analyzed in  $\text{CDCl}_3$  [37] and DFT/B3LYP/6-31+G(d,p) in gas phase and different solvent using CPCM model

molecular geometry, absorption maxima ( $\lambda_{\text{max}}$ ), oscillator strengths ( $f$ ), excitation energy ( $E_{\text{ex}}$ ), major contributions to electronic transitions and three major excitations of 4B2AEAB and its H-bonded derivatives. The UV-visible spectral analysis of 4B2AEAB and its derivatives were calculated by using TD-DFT method with 6-31+G(d,p) basis set in gas phase and solvent phase using CPCM model. The UV data and parameters are summarized in Table-5a and 5b. The UV-visible spectra of 4B2AEAB and its H-bonded derivatives (4B2AEAB4NP and 4B2AEABTU) are shown in Fig. 4a-c. From Table-5a, the theoretical absorption wavelength ( $\lambda_{\text{max}}$ ) at 354.16 nm has 0.0013 oscillator strength and major contribution is H-2 $\rightarrow$ L (93%), H $\rightarrow$ L (2%).

Another absorption wavelength in chloroform solvent is 343.74 nm with 0.0287 (O.S.) and major contribution of orbitals is H-3 $\rightarrow$ L (23%), H-2 $\rightarrow$ L (57%), H $\rightarrow$ L (16%) of the title molecule. The increasing order of wavelength ( $\lambda_{\text{max}}$ ) of

4B2AEAB are 354.16 nm > 343.74 nm > 342.64 nm > 342.18 nm > 341.88 nm in gas phase, chloroform, dichloromethane, dimethyl sulfoxide and water solvent, respectively. From Table-5b, it is observed that in donor- $\pi$ -acceptor adduct 4B2AEAB4NP molecule, the absorption wavelength ( $\lambda_{\text{max}}$ ) at 388 nm has 0.0152 oscillator strength and major contribution of HOMO and LUMO are H $\rightarrow$ L (99%) in water solvent. The  $\lambda_{\text{max}}$  of 4B2AEAB4NP molecule increasing order is water > gas phase. Another donor- $\pi$ -acceptor 4B2AEABTU molecule the wavelength ( $\lambda_{\text{max}}$ ) observed at 644.75 nm has 0.000 oscillator strength and the major contributions of orbitals are H $\rightarrow$ L (99%) in gas phase and 462.43 nm in water solvent has 0.0036 oscillator strength and the major contributions of frontier molecular orbitals (FMOs) are H $\rightarrow$ L (52%), H $\rightarrow$ L+1 (47%).

**Natural bond orbital (NBO) analysis:** NBO analysis has been performed on the title molecule at DFT/B3LYP/6-31+G(d,p) level of theory in the gas phase in order to explain inter and intramolecular interactions, charge transfer within the molecule, second order perturbation theory analysis of Fock matrix for the title molecule (4B2AEAB). NBO analysis gives an effective tool for studying ‘natural Lewis structure’ because all orbitals of molecule include the highest possible percentage of electron density (ED). NBOs also help in studying inter- and intramolecular interactions as well as charge transfer or conjugative interactions in different molecular systems [53]. The strength of delocalization interaction (or stabilization energy)  $E^{(2)}$  shows the strength of interaction in between electron donors and electron acceptors, *i.e.*, as the value of stabilization energy  $E^{(2)}$  increase the strength of interaction increase and *vice-versa*, more intensive is the interaction between donor and acceptor, the greater the extent of conjugation of the whole system. The stabilization energy  $E^{(2)}$  between donor and acceptor is resolved by utilizing the second order energy lowering relation as [54]:

TABLE-5a					
ABSORPTION SPECTRA DATA OBTAINED BY TD-DFT METHODS FOR THE TITLE MOLECULE (4B2AEAB) AT B3LYP/6-31+G (d, p) OPTIMIZED GEOMETRY IN THE GAS PHASE AND IN DIFFERENT SOLVENT PHASE USING CPCM MODEL					
$\lambda_{\text{max}}$ (nm)	$E_{\text{ex}}$ (eV)	(f)	Molecular orbital/character (HOMO=H, LUMO=L)	Excitation	
Water					
341.88	3.6266	0.0898	H-3 $\rightarrow$ L (38%), H-2 $\rightarrow$ L (13%), H $\rightarrow$ L (46%),	ES-1	
334.35	3.7082	0.1238	H-3 $\rightarrow$ L (43%), H $\rightarrow$ L (49%), H-2 $\rightarrow$ L (4%)	ES-2	
309.52	4.0057	0.0206	H-1 $\rightarrow$ L (92%), H $\rightarrow$ L+3 (3%)	ES-3	
DMSO					
342.18	3.6234	0.0963	H-3 $\rightarrow$ L (36%), H-2 $\rightarrow$ L (13%), H $\rightarrow$ L (47%)	ES-1	
334.69	3.7044	0.1263	H-3 $\rightarrow$ L (43%), H $\rightarrow$ L (48%), H-2 $\rightarrow$ L (5%)	ES-2	
309.60	4.0046	0.0219	H-1 $\rightarrow$ L (93%), H $\rightarrow$ L+3 (3%)	ES-3	
DCM					
342.64	3.6185	0.0538	H-3 $\rightarrow$ L (39%), H-2 $\rightarrow$ L (30%), H $\rightarrow$ L (28%)	ES-1	
334.23	3.7096	0.1708	H-3 $\rightarrow$ L (23%), H $\rightarrow$ L (67%), H-2 $\rightarrow$ L (7%)	ES-2	
308.22	4.0226	0.0218	H-1 $\rightarrow$ L (91%), H $\rightarrow$ L+3(3%)	ES-3	
Chloroform					
343.74	3.6069	0.0287	H-3 $\rightarrow$ L (23%), H-2 $\rightarrow$ L (57%), H $\rightarrow$ L (16%)	ES-1	
333.28	3.7201	0.1993	H $\rightarrow$ L (79%), H-3 $\rightarrow$ L (9%), H-2 $\rightarrow$ L (8%)	ES-2	
306.85	4.0406	0.0219	H-1 $\rightarrow$ L (91%), H $\rightarrow$ L+3 (3%)	ES-3	
Gas phase					
354.16	3.5008	0.0013	H-2 $\rightarrow$ L (93%), H $\rightarrow$ L (2%)	ES-1	
320.30	3.8709	0.1715	H $\rightarrow$ L (91%), H-3 $\rightarrow$ L (2%), H-1 $\rightarrow$ L (3%)	ES-2	
297.66	4.1653	0.0128	H-1 $\rightarrow$ L (86%), H $\rightarrow$ L+3 (6%), H $\rightarrow$ L (3%)	ES-3	

TABLE-5b					
ABSORPTION SPECTRA DATA OBTAINED BY TD-DFT METHODS FOR THE H-BONDED 4B2AEAB4NP AND 4B2AEABTU AT B3LYP/6-31+G (d, p) OPTIMIZED GEOMETRY IN THE GAS PHASE AND IN WATER SOLVENT PHASE USING CPCM MODEL					
$\lambda_{max}$ (nm)	$E_{ex}$ (eV)	(f)	Molecular orbital/character (HOMO=H, LUMO=L)	Excitation	
4B2AEAB4NP/Gas phase					
380.85	3.255	0.0202	H→L (95%)	ES-1	
352.36	3.518	0.0011	H-4→L+1 (95%)	ES-2	
346.76	3.575	0.2257	H-1→L (92%)	ES-3	
4B2AEAB4NP/Water Solvent					
388.00	3.195	0.0152	H→L (99%)	ES-1	
353.14	3.510	0.3827	H-2→L (23%), H→L+1 (72%)	ES-2	
343.96	3.604	0.1143	H-8→L (10%), H-2→L (58%) H→L+1 (21%)	ES-3	
4B2AEABTU/Gas phase					
644.75	1.923	0.000	H→L (99%)	ES-1	
456.87	2.713	0.0044	H→L+1 (41%), H→L+2 (57%)	ES-2	
421.57	2.941	0.0198	H-1→L (95%), H-4→L (2%)	ES-3	
4B2AEABTU/Water solvent					
462.43	2.681	0.0036	H→L (52%), H→L+1 (47%)	ES-1	
420.55	2.948	0.0024	H→L (47%), H→L+1 (52%)	ES-2	
362.69	3.418	0.2913	H-1→L (90%), H-5→L (2%), H-2→L (3%)	ES-3	

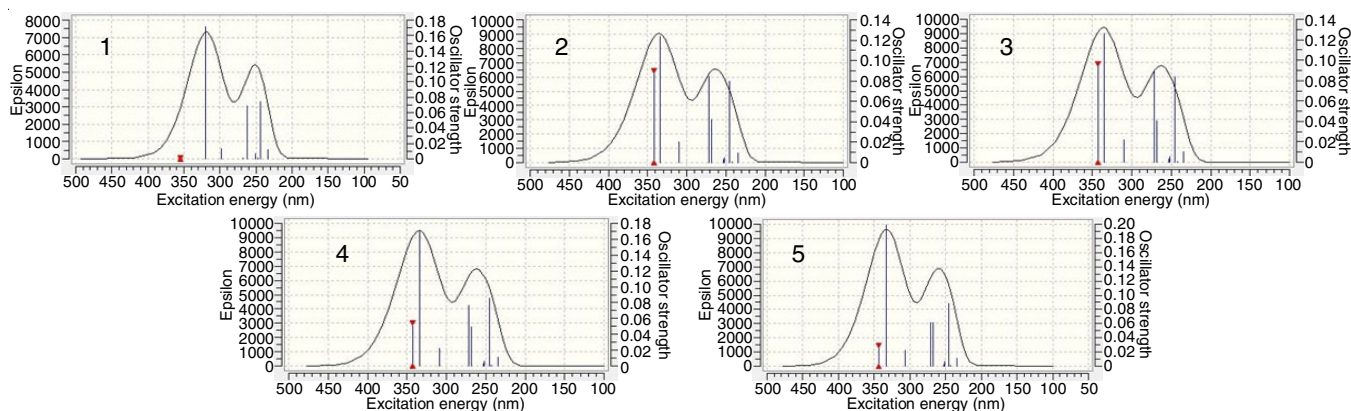


Fig. 4a. Comparative UV-vis spectra (1-5) of title molecule 4B2AEAB calculated at TD-DFT/B3LYP/6-31+G (d, p) in gas phase and different solvent using CPCM model

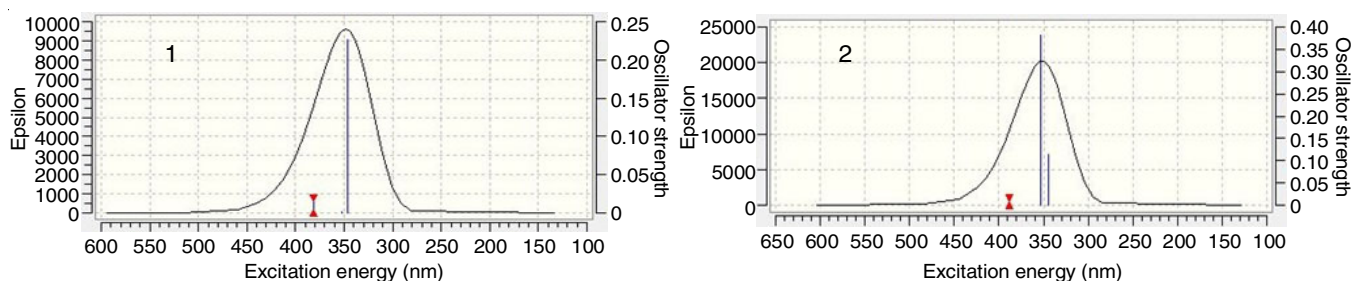


Fig. 4b. Comparative UV-vis spectra (1-2) of H-bonded 4B2AEAB4NP molecule calculated at TD-DFT/B3LYP/6-31+G (d, p) in gas phase and water solvent using CPCM model

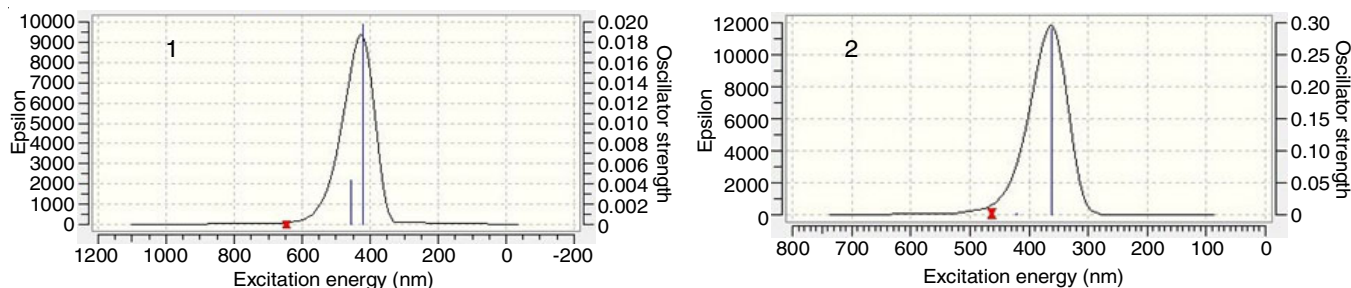


Fig. 4c. Comparative UV-vis spectra (1-2) of H-bonded 4B2AEABTU molecule calculated at TD-DFT/B3LYP/6-31+G (d, p) in gas phase and water solvent using CPCM model

$$E^{(2)} = \Delta E_{ij} = q_i \frac{(F_{ij})^2}{(E_j - E_i)} \quad (1)$$

where  $q_i$  is the donor orbital occupancy (or population of donor orbital), the off-diagonal Fock is asserted as  $F_{ij}$  or Kohn-Sham matrix element between  $i$  and  $j$  NBO orbitals. The results of second order perturbation theory analysis of Fock matrix for 4B2AEAB are listed in Table-6. NBO analysis of 4B2AEAB indicates the intramolecular interactions and interaction between donor and acceptor will be intense due to the increase of stabilization energy  $E^{(2)}$ . According to the stabilization energy  $E^{(2)}$  values of 4B2AEAB, the following transitions are occurred;  $\pi(C1-C2) \rightarrow \pi^*(C3-C4/C5-C6/C11-O12)$  (15.98/22.40/29.23 kcal/mol),  $\pi(C3-C4) \rightarrow \pi^*(C1-C2/C5-C6/C5-C6)$  (28.84/13.19/183.10 kcal/mol),  $\pi(C5-C6) \rightarrow \pi^*(C1-C2/C3-C4)$  (13.45/20.77 kcal/mol) and these transition take place within the benzene

ring of the title molecule (4B2AEAB). The  $\sigma(C21-H24) \rightarrow \pi^*(C20-O37)$  (4.66 kcal/mol) this transition reveals that it take place within the acetyl group of 4B2AEAB side chain molecule. In addition, the major transitions between lone pairs are also occurred;  $LP(2)O12 \rightarrow \sigma^*(C1-C11/C11-H13)$  (16.85/19.55 kcal/mol),  $LP(1) N35 \rightarrow \pi^*(C3-C4)$  (46.51 kcal/mol)  $\sigma^*(C14-C15/C25-C26)$  (6.43/6.73 kcal/mol),  $LP(1) \rightarrow \sigma^*(C20-O37)$  (8.92 kcal/mol),  $LP(2) O36 \rightarrow \pi^*(C20-O37)$  (50.35 kcal/mol),  $LP(2) O37 \rightarrow \sigma^*(C20-O36)$  (33.10 kcal/mol),  $LP(2) O38 \rightarrow \pi^*(C31-O39)$  (50.68 kcal/mol). The increasing order of maximum stabilization energy of transitions are  $\pi(C3-C4) \rightarrow \pi^*(C5-C6)$  (183.10 kcal/mol) >  $LP(2) O38 \rightarrow \pi^*(C31-O39)$  (50.68 kcal/mol) >  $LP(2) O36 \rightarrow \pi^*(C20-O37)$  (50.35 kcal/mol) >  $LP(1) N35 \rightarrow \pi^*(C3-C4)$  (46.51 kcal/mol). The larger stabilization energy shows the hyperconjugative interactions between electron donor groups to acceptor groups in 4B2AEAB molecule.

TABLE-6  
SECOND ORDER PERTURBATION ENERGIES  $E^{(2)}$  (Kcal/mol) CORRESPONDING TO THE MOST IMPORTANT CHARGE TRANSFER (DONOR-ACCEPTOR) IN 4B2AEAB STUDIED BY B3LYP/6-31+G (d, p) IN WATER SOLVENT USING CPCM MODEL

Donor (i)	Type	ED/e	Acceptor (j)	Type	ED/e	$E^{(2)}$ (Kcal/mol)	$E(j)-E(i)$ (a.u.)	$F(i, j)$ (a.u.)
C1-C2	$\sigma$	1.9756	C1-C6	$\sigma^*$	0.0253	3.05	1.25	0.055
C1-C2	$\sigma$	1.9756	C1-C11	$\sigma^*$	0.0523	1.45	1.17	0.037
C1-C2	$\sigma$	1.9756	C2-C3	$\sigma^*$	0.0118	2.21	1.28	0.048
C1-C2	$\sigma$	1.9756	C2-H7	$\sigma^*$	0.0131	0.86	1.17	0.028
C1-C2	$\sigma$	1.9756	C3-H8	$\sigma^*$	0.0139	2.27	1.17	0.046
C1-C2	$\sigma$	1.9756	C6-H10	$\sigma^*$	0.0135	2.24	1.17	0.046
C1-C2	$\sigma$	1.9756	C11-O12	$\sigma^*$	0.0041	2.07	1.26	0.046
C1-C2	$\pi$	1.6179	C1-C2	$\pi^*$	0.4331	1.69	0.27	0.019
C1-C2	$\pi$	1.6179	C3-C4	$\pi^*$	0.4252	15.98	0.26	0.059
C1-C2	$\pi$	1.6179	C5-C6	$\pi^*$	0.2711	22.40	0.28	0.072
C1-C2	$\pi$	1.6179	C11-O12	$\pi^*$	0.1898	29.23	0.25	0.080
C1-C6	$\sigma$	1.9745	C1-C2	$\sigma^*$	0.0217	3.04	1.25	0.055
C1-C6	$\sigma$	1.6745	C1-C11	$\sigma^*$	0.0523	1.77	1.17	0.041
C1-C6	$\sigma$	1.9745	C2-H7	$\sigma^*$	0.0131	2.25	1.16	0.046
C1-C6	$\sigma$	1.9745	C5-C6	$\sigma^*$	0.0116	2.24	1.29	0.048
C1-C6	$\sigma$	1.9745	C5-H9	$\sigma^*$	0.0128	2.31	1.17	0.047
C1-C6	$\sigma$	1.9745	C6-H10	$\sigma^*$	0.0135	0.88	1.17	0.029
C1-C6	$\sigma$	1.9745	C11-H13	$\sigma^*$	0.0560	1.06	1.10	0.031
C1-C11	$\sigma$	1.9844	C1-C2	$\sigma^*$	0.0217	2.07	1.24	0.045
C1-C11	$\sigma$	1.9844	C1-C6	$\sigma^*$	0.0253	2.12	1.24	0.046
C1-C11	$\sigma$	1.9844	C2-C3	$\sigma^*$	0.0118	2.06	1.27	0.046
C1-C11	$\sigma$	1.9844	C5-C6	$\sigma^*$	0.0116	2.04	1.28	0.046
C2-H7	$\sigma$	1.9791	C1-C6	$\sigma^*$	0.0253	4.39	1.08	0.062
C2-H7	$\sigma$	1.9791	C3-C4	$\sigma^*$	0.0219	4.58	1.05	0.062
C3-C4	$\sigma$	1.9738	C2-C3	$\sigma^*$	0.0118	2.34	1.29	0.049
C3-C4	$\sigma$	1.9738	C2-H7	$\sigma^*$	0.0131	2.16	1.17	0.045
C3-C4	$\sigma$	1.9738	C4-C5	$\sigma^*$	0.0228	2.57	1.22	0.050
C3-C4	$\sigma$	1.9738	C4-N35	$\sigma^*$	0.0295	1.26	1.16	0.034
C3-C4	$\sigma$	1.9738	C5-H9	$\sigma^*$	0.0128	2.21	1.17	0.046
C3-C4	$\sigma$	1.9738	C14-N35	$\sigma^*$	0.0203	3.39	1.03	0.053
C3-C4	$\pi$	1.5769	C1-C2	$\pi^*$	0.4331	28.84	0.28	0.080
C3-C4	$\pi$	1.5769	C3-C4	$\pi^*$	0.4252	1.50	0.27	0.018
C3-C4	$\pi$	1.5769	C5-C6	$\pi^*$	0.2711	13.19	0.28	0.057
C3-H8	$\sigma$	1.9772	C1-C2	$\sigma^*$	0.0217	3.99	1.08	0.059
C3-H8	$\sigma$	1.9772	C4-C5	$\sigma^*$	0.0228	4.16	1.04	0.059
C4-C5	$\sigma$	1.9733	C3-C4	$\sigma^*$	0.0219	2.55	1.22	0.050
C4-C5	$\sigma$	1.9733	C3-H8	$\sigma^*$	0.0139	2.21	1.18	0.046
C4-C5	$\sigma$	1.9733	C4-N35	$\sigma^*$	0.0295	1.18	1.16	0.033
C4-C5	$\sigma$	1.9733	C5-C6	$\sigma^*$	0.0116	2.36	1.29	0.049
C4-C5	$\sigma$	1.9733	C6-H10	$\sigma^*$	0.0135	2.12	1.18	0.045
C4-C5	$\sigma$	1.9733	C25-N35	$\sigma^*$	0.0258	3.49	1.03	0.053

C4-N35	$\sigma$	1.9866	C14-N35	$\sigma^*$	0.0203	1.13	1.16	0.032
C4-N35	$\sigma$	1.9866	C25-N35	$\sigma^*$	0.0258	1.11	1.15	0.032
C5-C6	$\sigma$	1.9793	C1-C6	$\sigma^*$	0.0253	2.60	1.27	0.051
C5-C6	$\sigma$	1.9793	C1-C11	$\sigma^*$	0.0523	3.09	1.19	0.055
C5-C6	$\sigma$	1.9793	C4-C5	$\sigma^*$	0.0228	2.56	1.23	0.050
C5-C6	$\sigma$	1.9793	C4-N35	$\sigma^*$	0.0295	3.70	1.18	0.059
C5-C6	$\sigma$	1.9793	C5-H9	$\sigma^*$	0.0128	1.43	1.19	0.037
C5-C6	$\pi$	1.7338	C1-C2	$\pi^*$	0.4331	13.45	0.28	0.058
C5-C6	$\pi$	1.7338	C3-C4	$\pi^*$	0.4252	20.77	0.27	0.070
C5-H9	$\sigma$	1.9779	C1-C6	$\sigma^*$	0.0253	3.95	1.08	0.058
C5-H9	$\sigma$	1.9779	C3-C4	$\sigma^*$	0.0219	4.02	1.06	0.058
C6-H10	$\sigma$	1.9794	C1-C2	$\sigma^*$	0.0217	4.40	1.08	0.062
C6-H10	$\sigma$	1.9794	C4-C5	$\sigma^*$	0.0228	4.67	1.04	0.062
C11-O12	$\pi$	1.9836	C1-C2	$\pi^*$	0.4331	4.26	0.40	0.041
C11-H13	$\sigma$	1.9858	C1-C6	$\sigma^*$	0.0253	5.00	1.09	0.066
C14-C15	$\sigma$	1.9854	C20-O36	$\sigma^*$	0.1007	1.78	0.99	0.038
C14-C15	$\sigma$	1.9854	C25-N35	$\sigma^*$	0.0258	1.05	0.96	0.028
C14-H16	$\sigma$	1.9816	C4-N35	$\sigma^*$	0.0295	3.90	0.99	0.056
C14-N35	$\sigma$	1.9833	C3-C4	$\sigma^*$	0.0219	3.06	1.26	0.056
C15-O36	$\sigma$	1.9879	C14-N35	$\sigma^*$	0.0203	1.91	1.16	0.042
C15-O36	$\sigma$	1.9879	C20-C21	$\sigma^*$	0.0478	2.53	1.20	0.050
C20-C21	$\sigma$	1.9844	C15-O36	$\sigma^*$	0.0264	3.59	0.91	0.051
C21-H22	$\sigma$	1.9860	C20-O36	$\sigma^*$	0.1007	4.88	0.87	0.060
C21-H23	$\sigma$	1.9860	C20-O37	$\sigma^*$	0.0254	5.24	0.51	0.048
C21-H24	$\sigma$	1.9860	C20-O37	$\sigma^*$	0.0254	3.28	1.09	0.053
C21-H24	$\sigma$	1.9860	C20-O37	$\pi^*$	0.2301	4.66	0.51	0.046
O12	LP(2)	1.8988	C1-C11	$\sigma^*$	0.0523	16.85	0.75	0.102
O12	LP(2)	1.8988	C11-H13	$\sigma^*$	0.0560	19.55	0.68	0.104
N35	LP(1)	1.6936	C3-C4	$\pi^*$	0.4252	46.51	0.27	0.102
N35	LP(1)	1.6936	C14-C15	$\sigma^*$	0.0234	6.43	0.62	0.061
N35	LP(1)	1.6936	C14-H17	$\sigma^*$	0.0204	3.70	0.68	0.048
N35	LP(1)	1.6936	C15-O36	$\sigma^*$	0.0264	1.21	0.50	0.024
N35	LP(1)	1.6936	C25-C26	$\sigma^*$	0.0254	6.73	0.62	0.062
N35	LP(1)	1.6936	C25-H27	$\sigma^*$	0.0133	2.60	0.68	0.041
O36	LP(1)	1.9613	C20-O37	$\sigma^*$	0.0254	8.92	1.16	0.091
O36	LP(2)	1.7919	C20-O37	$\pi^*$	0.2301	50.35	0.33	0.115
O37	LP(2)	1.8628	C20-C21	$\sigma^*$	0.0478	16.87	0.65	0.096
O37	LP(2)	1.8628	C20-O36	$\sigma^*$	0.1007	33.10	0.64	0.131
O38	LP(1)	1.9597	C31-O39	$\sigma^*$	0.0254	8.86	1.16	0.091
O38	LP(2)	1.7900	C31-O39	$\pi^*$	0.2313	50.68	0.33	0.116
O39	LP(2)	1.8639	C31-C32	$\sigma^*$	0.0479	16.83	0.65	0.096
O39	LP(2)	1.8639	C31-O38	$\sigma^*$	0.1001	33.02	0.64	0.131
C3-C4	$\pi$	1.5769	C5-C6	$\pi^*$	0.2711	183.10	0.01	0.077

Note:  ${}^aE^{(2)}$  means energy of hyper-conjugative interaction (stabilization energy),  ${}^bE(j)-E(i)$  means energy difference between donor and acceptor I and j NBO orbitals,  ${}^cF(i, j)$  is the Fock matrix element between I and j NBO orbitals.

### Local reactivity descriptors: Fukui function analysis

**(FFA):** The chemical potential ( $\mu$ ), chemical hardness ( $\eta$ ), electronegativity ( $\chi$ ), electrophilicity ( $\omega$ ) and softness ( $S$ ) are the global reactivity properties related to the chemical reactivity and where as local reactivity is related to selectivity postulation. So Fukui function analysis is the most important parameter of local reactivity. The Fukui function analysis for molecule defined the derivatives of electron density with respect to the change in number of electrons, keeping the location of nuclei unaltered [55,56]. Fukui function analysis gives us information about highly nucleophilic and electrophilic positions in a molecules or compounds. In employed appropriate way of calculating the Fukui function at atomic purpose is to use the condensed Fukui functions [57]. The Fukui function  $f_k^+(r)$  for nucleophilic attacks ( $r$ ),  $f_k^-(r)$  for electro-philic attacks ( $r$ ) and  $f_k^0(r)$  for free radical attacks ( $r$ ) can be mathematically expressed as:

For nucleophilic attacks:

$$f_k^+(r) = q_k(r) (N + 1) - q_k(r) (N) \quad (2)$$

For electrophilic attacks:

$$f_k^-(r) = q_k(r) (N) - q_k(r) (N-1) \quad (3)$$

For free radical attacks:

$$f_k^0(r) = q_k(r) (N+1) - q_k(r) (N-1) \quad (4)$$

In above equations,  $q_k$  is the atomic charge (evaluated from Mulliken charges) at  $k^{\text{th}}$  atomic site in the cationic ( $N-1$ ), anionic ( $N+1$ ) or neutral molecule ( $N$ ). Roy *et al.* [58] gives hypothesis of the “relative nucleophilicity” ( $S_k^-/S_k^+$ ) and the “relative electrophilicity” ( $S_k^+/S_k^-$ ) descriptor for  $k^{\text{th}}$  atoms and this indicates preferred nucleophilic and electrophilic reactive positions in molecule for the study of the intermolecular reactivity in the chemical compounds. The nucleophilic and the elec-

trophilic local softness  $s_k^-$  and  $s_k^+$  [55] can be represented using mathematical equations as given below:

Nucleophilic local softness:

$$s_k^- = S f_k^- \quad (5)$$

Electrophilic local softness:

$$s_k^+ = S f_k^+ \quad (6)$$

In the above equation  $S$  is the chemical softness and  $f_k^-$  and  $f_k^+$  are the nucleophilic and electrophilic Fukui functions.

Chattaraj *et al.* [59] proposed the postulation of generalized philicity  $\omega_k^x$  ( $x = -, +$  or  $0$ ) indices to identify the most reactive nucleophilic, electrophilic and radical positions in molecule and regioselectivity studies of chemical compounds. The local (or condensed) nucleophilicity  $\omega_k^-$  and electrophilicity  $\omega_k^+$  indices are related to the Parr global electrophilicity index ( $\omega$ ) and the corresponding Fukui functions by eqns. 7 and 8 are given below:

Local nucleophilicity:

$$\omega_k^- = \omega f_k^- \quad (7)$$

Local electrophilicity:

$$\omega_k^+ = \omega f_k^+ \quad (8)$$

where  $\omega$  is the global electrophilicity index and  $f_k^-$  and  $f_k^+$  are the nucleophilic and electrophilic Fukui functions. According to the Parr and Yang stated that sites in chemical compound or reactant with largest values of Fukui function ( $f_k$ ) represent the high reactivity for corresponding attacks as compared to other atomic sites in the molecule or reactant. In the present study, the values of calculated Fukui functions ( $f_k$ ) based on the Mulliken atomic charges and calculated at DFT method with B3LYP and B3PW91 with 6-31+G(d,p) basis set in the water solvent using CPCM model, given in the Table-7a and 7b.

From Table-7a and 7b, it is clear that the most preferred nucleophilic attack site in 4B2AEAB order at B3LYP and B3PW91 level are  $6C > 2C > 11C > 14C > 15C > 25C$  and  $6C > 2C > 15C > 25C > 14C > 11C$ , respectively. The most preferred electrophilic attack site order in 4B2AEAB at B3LYP and B3PW91 are same  $4C > 5C > 26C > 12O > 35N$ . The maximum value order of nucleophilic local softness ( $s_k^-$ ) of 4B2AEAB at B3LYP and B3PW91 level are  $6C > 2C > 11C > 14C > 15C > 25C$  and  $6C > 2C > 15C > 25C > 11C > 14C > 12O$ , respectively. The maximum value of electrophilic local softness ( $s_k^+$ ) order of 4B2AEAB at B3LYP and B3PW91 level are  $4C > 5C > 20C > 11C > 1C > 26C$  and  $4C > 5C > 1C > 26C > 20C$ , respectively. The maximum value of local electrophilicity ( $\omega^+$ ) order at B3LYP and B3PW91 level are  $6C > 2C > 11C > 14C > 15C > 25C$  and  $6C > 2C > 15C > 25C > 11C > 14C > 12O$ , respectively. The maximum value orders of local nucleophilicity ( $\omega_k^-$ ) of 4B2AEAB at B3LYP and B3PW91 level are  $C4 > C5 > C1 > C26 > O12 > N35 > C20 > C31 > C11 > O36$  and  $C4 > C5 > C1 > C26 > O12 > N35 > C3 > C20 > C31 > O36 > C11$ , respectively and these sites are more labile for electrophilic attacks. The increasing order of local electrophilicity at B3LYP and B3PW91 are  $C6 > C2 > C11 > C15 > C25 > C21 > O39$  and  $C6 > C2 > C15 > C25 > C11 > C14 > O12 > C32 > O39 > N35$ , respectively and these sites are more labile for nucleophilic attacks.

**Electric moments [non-linear optical (NLO) properties calculations]:** The theoretical calculation helps in easily understood the non-linear optical behaviour of NLO active materials. The intermolecular charge transfer and hyperpolarizability is the best chemical phenomenon play very important role to explain the participation of molecular structure or geometry in non-linear optical properties of NLO active molecule. Therefore, the molecular structure and NLO properties, both

TABLE-7a  
FUKUI FUNCTION VALUES ON THE BASIS OF THE MULLIKEN ATOMIC CHARGES OF NEUTRAL, CATION AND ANION, THE FUKUI FUNCTIONS ( $f_k^+$ ,  $f_k^-$ ), LOCAL SOFTNESS ( $s_k^+$ ,  $s_k^-$ ) AND LOCAL PHILICITY ( $\omega_k^+$ ,  $\omega_k^-$ ) OF 4B2AEAB CALCULATED AT DFT/B3LYP/6-31+G (d, p) BASIS SET IN THE WATER SOLVENT USING CPCM MODEL

Atoms	(N)	(N+1)	(N-1)	$f_{(r)}^+$	$f_{(r)}^-$	$s_k^+$	$s_k^-$	$\omega_k^+$	$\omega_k^-$
1C	0.4474	0.4101	0.2471	-0.0372	0.2002	-0.0090	0.0487	-0.1375	0.7403
2C	-1.0053	-0.5952	-0.5775	0.4101	-0.4277	0.0998	-0.1041	1.5165	-1.5816
3C	0.4246	0.4390	0.4733	0.0143	-0.0486	0.0034	-0.0118	0.0528	-0.1797
4C	-0.3073	-0.7736	-1.1516	-0.4662	0.8442	-0.1135	0.2055	-1.7240	3.1218
5C	0.5204	0.2156	0.0832	-0.3048	0.4372	-0.0742	0.1064	-1.1271	1.6167
6C	-0.2509	0.3698	0.0222	0.6207	-0.2286	0.1511	-0.0556	2.2953	-0.8453
11C	0.1890	0.3741	0.1225	0.1851	0.0664	0.0450	0.0556	0.6844	0.2455
12O	-0.5044	-0.3901	-0.6745	0.1142	0.1701	0.0278	0.0161	0.4223	0.6290
14C	0.0589	0.2388	0.1321	0.1799	-0.0731	0.0438	-0.0414	0.6652	-0.2703
15C	0.1191	0.2934	0.4006	0.1743	-0.2815	0.0424	-0.0178	0.6445	-1.0409
20C	0.6511	0.5369	0.5497	-0.1142	0.1014	-0.0278	0.0685	-0.4223	0.3749
21C	0.0436	0.0917	0.8441	0.0480	-0.0850	0.0116	-0.0246	0.1775	-0.3143
25C	0.1348	0.2989	0.1287	0.1640	0.0061	0.0399	0.0014	0.6064	0.0225
26C	0.3922	0.2553	0.2088	-0.1369	0.1833	-0.0333	0.0446	-0.5062	0.6778
31C	0.5697	0.5119	0.4856	-0.0577	0.0841	-0.0140	0.0204	-0.2133	0.3110
32C	0.0555	0.1502	0.1571	-0.0068	-0.1015	-0.0016	-0.0247	-0.0251	-0.3753
35N	0.0704	-0.1113	0.0394	-0.5058	0.1099	-0.1231	0.0267	-1.8704	0.4064
36O	-0.2613	-0.3114	-0.3206	0.0092	0.0592	0.0022	0.0144	0.0340	0.2189
37O	-0.5351	-0.4777	-0.4903	0.0125	-0.0447	0.0030	-0.0108	0.0462	-0.1653
38O	-0.2863	-0.2929	-0.2986	0.0056	0.0123	0.0013	0.0030	0.0207	0.0454
39O	-0.5264	-0.4564	-0.4984	0.0419	-0.0280	0.0102	-0.0068	0.1549	-0.1035

TABLE-7b  
 FUKUI FUNCTION VALUES ON THE BASIS OF THE MULLIKEN ATOMIC CHARGES OF NEUTRAL, CATION AND ANION, THE FUKUI FUNCTIONS ( $f_i^+$ ,  $f_i^-$ ), LOCAL SOFTNESS ( $s_k^+$ ,  $s_k^-$ ) AND LOCAL PHILICITY ( $\omega_k^+$ ,  $\omega_k^-$ ) OF THE TITLE MOLECULE (4B2AEAB) CALCULATED AT DFT/B3PW91/6-31+G (d, p) BASIS SET IN THE WATER SOLVENT USING CPCM MODEL

Atoms	(N)	(N+1)	(N-1)	$f_{(i)}^+$	$f_{(i)}^-$	$s_k^+$	$s_k^-$	$\omega_r^+$	$\omega_r^-$
1C	0.4631	0.4345	0.2203	-0.0586	0.2428	-0.0283	0.5020	-0.2188	0.9066
2C	-1.1739	-0.6735	-0.6185	0.5003	-0.5554	0.2416	-1.1483	1.8681	-2.0738
3C	0.5232	0.4155	0.4423	-0.1076	0.0809	-0.0519	0.1673	-0.4017	0.3020
4C	-0.4743	-0.7832	-1.1222	-0.3088	0.6478	-0.1491	1.3393	-1.1530	2.4188
5C	0.6130	0.2069	0.0741	-0.4061	0.5388	-0.1961	1.1140	-1.5163	2.0118
6C	-0.1999	0.4119	0.0144	0.6118	-0.2143	0.2954	-0.4430	2.2844	-0.8001
11C	0.1652	0.3259	0.1126	0.1607	0.0526	0.0776	0.1087	0.6000	0.1964
12O	-0.4785	-0.3699	-0.6596	0.1086	0.1810	0.0524	0.3742	0.4055	0.6758
14C	0.1062	0.2176	0.1237	0.1113	-0.0174	0.0537	-0.0359	0.4155	-0.0653
15C	0.0468	0.2671	0.3606	0.2203	-0.3138	0.1064	-0.6488	0.8226	-1.1717
20C	0.5668	0.4799	0.4927	-0.0868	0.0740	-0.0419	0.1530	-0.3241	0.2763
21C	0.0774	0.0991	0.0918	0.0217	-0.0144	0.0104	-0.0297	0.0810	-0.0537
25C	0.1634	0.3430	0.1871	0.1795	-0.0236	0.0866	-0.0487	0.6702	-0.0881
26C	0.3718	0.2402	0.1835	-0.1315	0.1883	-0.0635	0.3893	-0.4910	0.7031
31C	0.4700	0.4229	0.3974	-0.0471	0.0725	-0.0227	0.1499	-0.1758	0.2707
32C	0.0878	0.1652	0.1726	0.0774	-0.0848	0.0373	-0.1753	0.2890	-0.3166
35N	0.1488	0.1948	0.0002	0.0459	0.1486	0.0221	0.3072	0.1713	0.5548
36O	-0.2178	-0.2748	-0.2844	-0.0570	0.0666	-0.0275	0.1377	-0.2128	0.2486
37O	-0.5125	-0.4536	-0.4665	-0.2410	-0.046	-0.1164	-0.0951	-0.8998	-0.1717
38O	-0.2435	-0.2379	-0.2478	0.0055	0.0043	0.0026	0.0090	0.0205	0.0160
39O	-0.5035	-0.4320	-0.4747	0.0714	-0.0287	0.0344	-0.0594	0.2666	-0.1071

properties are correlated by theoretical method may suggest the possibilities of design and synthesis of novel non-linear optical (NLO) materials.

The electron cloud of atoms or molecule has the ability to interact with an external electric field and hence increases the asymmetric electronic distribution in the ground state and excited states of atoms or molecule, which increase the optical non-linearity of the molecular system [60]. An organic compound with enhanced NLO property include of a D- $\pi$ -A conjugation system substituted by an electron donor groups on one end and electron acceptor group on other end, forming a push-pull conjugated structure [61]. The first hyperpolarizability ( $\beta$ ) is a 3<sup>rd</sup> rank tensor that can be explained by  $3 \times 3 \times 3$  matrices. With the help of Kleinman symmetry the 27 components of the 3D-matrix reduced in to 10 components [62]. The components of  $\beta$  are explained as the coefficients in the Taylor series expansion of energy in the external electric field. When the external electric field is homogeneous and weak, this expansion becomes as:

$$E = E^0 - \mu F - 1/2\alpha F^2 - 1/6\beta F^3 - 1/24\gamma F^4 \quad (9)$$

where E is the external electric field,  $E^0$  is the energy of unperturbed molecule, F is the field at the origin,  $\mu$  is the dipole moment,  $\alpha$  is the polarizability,  $\beta$  and  $\gamma$  is the first hyperpolarizability and the second hyperpolarizability, respectively. The second hyperpolarizability is known as third order non-linear optical (NLO) coefficient and defined by forth rank tensor. The mathematical equations of electronic moments like total static dipole moment ( $\mu$ ), the average polarizability ( $\alpha$ ), anisotropy of polarizability and first hyperpolarizability ( $\beta_{tot}$ ) of the title molecule and its derivatives are defined by the x, y, z components given as:

$$\mu = (\mu_x^2 + \mu_y^2 + \mu_z^2)^{1/2} \quad (10)$$

$$\alpha = 1/3(\alpha_{xx} + \alpha_{yy} + \alpha_{zz}) \quad (11)$$

$$\Delta\alpha = \sqrt{[(\alpha_{xx} - \alpha_{yy})^2 + (\alpha_{xx} - \alpha_{zz})^2 + (\alpha_{yy} - \alpha_{zz})^2 + 6(\alpha_{xx}^2 + \alpha_{yy}^2 + \alpha_{zz}^2)]/2} \quad (12)$$

$$\beta_{tot} = [(\beta_{xxx} + \beta_{yyy} + \beta_{zzz})^2 + (\beta_{yyy} + \beta_{yxx} + \beta_{yzz})^2 + (\beta_{zzz} + \beta_{zxx} + \beta_{zyy})^2]^{1/2} \quad (13)$$

$$\beta_{tot} = [\beta_x^2 + \beta_y^2 + \beta_z^2]^{1/2} \quad (14)$$

where  $\beta_x^2$ ,  $\beta_y^2$ ,  $\beta_z^2$  are the components of the second order polarizability tensor and can be calculated by following equations:

$$\beta_i = \beta_{iii} + \frac{1}{3} \sum_{i \neq j} [(\beta_{ijj} + \beta_{jij} + \beta_{jji})], i, j = x, y, z \quad (15)$$

and average value of third-order hyperpolarizability is given by following equation:

$$\langle \gamma \rangle = \frac{1}{5} [\gamma_{xxxx} + \gamma_{yyyy} + \gamma_{zzzz} + 2(\gamma_{xyxy} + \gamma_{xxzz} + \gamma_{yyzz})] \quad (16)$$

To gain insight into the fundamental non-linear optical (NLO) properties like dipole moment ( $\mu$ ), polarizability ( $\alpha$ ), anisotropy of polarizability ( $\Delta\alpha$ ), first-order hyperpolarizability ( $\beta_{tot}$ ) and second-order hyperpolarizability ( $\langle \gamma \rangle$ ) and NLO response of novel organic NLO materials like 4B2AEAB, 4B2AEAB4NP and 4B2AEABTU compounds were calculated using DFT method with B3LYP and B3PW91 functional with 6-31+G(d,p) basis set in water solvent phase using CPCM model and presented in Table-8a. All the values of polarizability ( $\alpha$ ), hyperpolarizability ( $\beta$ ) and the Gaussian output file ( $\gamma$ ) are obtained in atomic units (a.u.), the calculated values have been converted into e.s.u. unit system ( $\alpha$ : 1 a.u. = 0.1482

$\times 10^{-24}$  esu;  $\beta$ : 1 a.u. =  $8.6393 \times 10^{-34}$  esu;  $\gamma$ : 1 a.u. =  $5.036 \times 10^{-40}$  esu). The calculated values of electronic moments are dipole moment ( $\mu$ ) 8.1514 and 8.0302 Debye, polarizability ( $\alpha$ )  $42.929 \times 10^{-24}$  and  $42.289 \times 10^{-24}$  esu, anisotropy of polarizability ( $\Delta\alpha$ )  $17.730 \times 10^{-24}$  and  $17.910 \times 10^{-24}$  esu, first-order hyperpolarizability ( $\beta_{\text{tot}}$ )  $2.80538 \times 10^{-30}$  and  $2.12040 \times 10^{-30}$  esu and second-order hyperpolarizability  $\langle\gamma\rangle$   $-2.05599 \times 10^{-36}$  esu and  $-2.00746 \times 10^{-36}$  esu) for title molecule (4B2AEAB) at B3LYP and B3PW91 with 6-31+ (d, p) basis set in water solvent, respectively.

The calculated dipole moment, polarizability, anisotropy of polarizability, first-order hyperpolarizability and second-order hyperpolarizability of 4B2AEAB4NP and 4B2AEABTU hydrogen bonded complex at B3LYP/6-31+G(d,p) basis set in water solvent using CPCM model values are 18.9971 Debye,  $65.0212186 \times 10^{-24}$  esu,  $39.1170235 \times 10^{-24}$  esu,  $12.73333 \times 10^{-30}$  esu,  $-8.02090806 \times 10^{-36}$  esu and 17.2703 Debye, 54.3673182  $\times 10^{-24}$  esu, 29.6642781  $\times 10^{-24}$  esu,  $12.00412 \times 10^{-30}$  esu,  $-5.52491331 \times 10^{-36}$  esu, respectively.

Further, the calculated values of 4B2AEAB and its derivatives were compared to the few known organic non-linear optical materials given in the literature such as 4-dimethyl amino benzaldehyde 4-nitrophenol complex (4DMAB4NP) [32], 1,2-dichloro-4-nitrobenzene (DCNB) [63], 3-aminopyridine-4-nitrophenol (3AP4NP) [64], 8-hydroxyquinolinium-3,5-dinitrobenzoate (HOQDNB) [65], morpholinium-2-chloro-4-nitrobenzoate (M2C4N) [66], 2-amino-4-picolinium-nitrophenolate nitrophenol (2A4PNN) [67], *N*-succinopyridine (NSP) [68], piperidinium *p*-hydroxybenzoate (PDPHB) [69], pyrrolidinium *p*-hydroxybenzoate (PYPHB) [70] and are listed in Table-8b.

The second-order hyperpolarizability value of 4B2AEAB and its derivatives (4B2AEAB4NP and 4B2AEABTU) depends on the numbers of factors, which include the extent of electronic conjugation, the nature of substituent and the dimensionality of the molecules. In these compounds, the presence of -CHO,  $-\text{N}(\text{C}_2\text{H}_4\text{-O-CO-CH}_3)_2$ , -OH group, -NO<sub>2</sub> are attached to the benzene rings; -NH<sub>2</sub> group and C=S group found in urea acted as donor- $\pi$ -acceptor system, which is responsible for the delo-

TABLE-8a  
THEORETICAL VALUES OF DIPOLE MOMENT ( $\mu$ ), POLARIZABILITY ( $\alpha$ ), ANISOTROPY OF POLARIZABILITY ( $\Delta\alpha$ ), FIRST-ORDER HYPERPOLARIZABILITY ( $\beta_{\text{tot}}$ ) AND SECOND-ORDER HYPERPOLARIZABILITY ( $\gamma$ ) FOR THE TITLE MOLECULE (4B2AEAB) AND ITS DERIVATIVES CALCULATED AT B3LYP/B3PW91 WITH 6-31+G (d, p) BASIS SET IN WATER SOLVENT USING CPCM MODEL

Dipole moment ( $\mu$ )	4B2AEAB B3LYP/B3PW91	4B2AEAB4NP B3LYP	4B2AEABTU B3LYP
$\mu_x$	4.0749/4.2396	17.0490	15.3377
$\mu_y$	2.9596/2.8681	-4.9738	-4.3201
$\mu_z$	6.4095/6.1874	-6.7440	-6.6599
$\mu_{\text{tot}}$	8.1514/8.0302	18.9971	17.2702
Polarizability ( $\alpha$ )	B3LYP/B3PW91	B3LYP	B3LYP
$\alpha_{xx}$ (a.u.)	364.552/361.879	597.876	490.999
$\alpha_{yy}$ (a.u.)	276.036/268.928	424.206	347.152
$\alpha_{zz}$ (a.u.)	228.438/225.260	294.137	262.402
$\alpha_{xy}$ (a.u.)	34.577/30.632	2.589	24.023
$\alpha_{xz}$ (a.u.)	55.190/56.614	-35.399	-39.942
$\alpha_{yz}$ (a.u.)	19.757/15.672	23.359	-15.397
$\alpha_{\text{tot}}$ (esu)	42.929/42.289	65.0212186	54.3673182
$\Delta\alpha$ (esu)	17.730/17.910	39.1170235	29.6642781
First-order hyperpolarizability ( $\beta$ )	B3LYP/B3PW91	B3LYP	B3LYP
$\beta_{xxx}$ (a.u.)	225.777/232.186	1177.1495	1246.5142
$\beta_{yyy}$ (a.u.)	-36.551/-40.154	15.0324	27.0674
$\beta_{zzz}$ (a.u.)	20.991/20.151	14.1851	-10.5404
$\beta_{xxy}$ (a.u.)	82.30870.404	-269.8822	-191.3447
$\beta_{xyy}$ (a.u.)	52.795/41.695	174.0583	51.8873
$\beta_{xxz}$ (a.u.)	82.619/77.466	-420.4723	-203.1554
$\beta_{xyz}$ (a.u.)	31.138/24.636	30.9610	7.5343
$\beta_{vyz}$ (a.u.)	20.794/16.241	-50.5603	-21.1483
$\beta_{xzz}$ (a.u.)	6.219/10.484	21.9843	55.5730
$\beta_{yzz}$ (a.u.)	48.376/48.884	-24.3819	-41.2787
$\beta_{\text{tot}}$ (esu) ( $\times 10^{-30}$ )	2.80538/2.12040	12.73333	12.00412
Second-order hyperpolarizability $\langle\gamma\rangle$	B3LYP/B3PW91	B3LYP	B3LYP
$\gamma_{xxxx}$ (a.u.)	-6644.675// -6714.022	-44747.2965	-32380.6452
$\gamma_{yyyy}$ (a.u.)	-4316.963/ -4067.100	-4789.0657	-4128.7302
$\gamma_{zzzz}$ (a.u.)	-1002.040/ -985.096	-1908.7551	-1263.3180
$\gamma_{xxyy}$ (a.u.)	-2058.897/ -1978.235	-6541.3822	-3816.9938
$\gamma_{xxzz}$ (a.u.)	-1342.987/ -1301.509	-6257.2923	-3626.9311
$\gamma_{yyzz}$ (a.u.)	-822.781/ -802.694	-1296.6178	-1096.8198
$\langle\gamma\rangle$ ( $\times 10^{-36}$ esu)	-2.05599/ -2.00746	-8.02090806	-5.52491331

calization of electron and conjugation within the molecule. This electron delocalization in turn induces non-linear optical (NLO) behaviour in 4B2AEAB, 4B2AEAB4NP and 4B2AEABTU compounds.

**Frontier molecular orbital (FMOs) analysis:** The transition of electron from the ground state to the first excited state is mainly explained by the excitation from HOMO (highest occupied molecular orbital) to the LUMO (lowest unoccupied molecular orbital) FMOs (HOMO and LUMO) are the main orbitals having most important contribution in stability [71] and their distinct properties such as energy gap and electron density are important for researchers to study the physico-chemical properties of the molecule [68]. The HOMO and LUMO transitions can be easily understood from the visualization of orbital charge distribution over the 4B2AEAB and its derivatives. The HOMO and LUMO is represented by electron donor and electron acceptor, respectively. The energies of HOMO, LUMO and energy gap ( $\Delta E_{\text{gap}}$ ) of 4B2AEAB, 4B2AEAB4NP and 4B2AEABTU compounds are shown in Fig. 5. In order to find out the information about chemical reactivity of 4B2AEAB and its derivatives, the global reactivity descriptors such as  $E_{\text{HOMO}}$ ,  $E_{\text{LUMO}}$ , energy gap ( $\Delta E_{\text{L-H}}$ ), chemical hardness ( $\eta$ ), electronegativity ( $\chi$ ), chemical potential ( $\mu$ ), global softness, electrophilicity index ( $\omega$ ) and maximum amount of electronic charge that an electrophile may accept ( $Q_{\text{max}}$ ) have

been calculated by using HOMO and LUMO energies and calculated at DFT/B3LYP & B3PW91/6-31+G(d,p) in water solvent using CPCM model. The mathematical equations (17-25) of global reactivity descriptors [72-75] and results are shown in Table-9.

From Table-9, the frontier orbital gap of 4B2AEAB at B3LYP and B3PW91 level are 4.106 eV and 4.135 eV, respectively. The lowest energy gap found in 4B2AEAB4NP compound shows a high chemical reactivity and low kinetic stability and termed as soft molecule. The lowest energy gap order of 4B2AEAB4NP, 4B2AEABTU and 4B2AEAB at B3LYP level are  $3.229 > 3.980 > 4.106$ , respectively. The value of electrophilicity index of 4B2AEAB and its H-bonded derivatives (4B2AEAB4NP, 4B2AEABTU) at B3LYP level of theory are 3.698 eV and 6.2153 eV, 4.1391 eV, respectively and the energy lowering due to maximal flow of electrons found between donor and acceptor of 4B2AEAB4NP molecule. The value of  $Q_{\text{max}}$  of 4B2AEAB, 4B2AEAB4NP and 4B2AEABTU at B3LYP level are 1.898 and 2.7743, 2.0394, respectively, the 4B2AEAB4NP compound shows the maximum amount of electronic charge transfer between donor and acceptor.

In addition, as a result, global reactivity descriptors, chemical potential, hardness, global softness and electrophilicity index showed that the title molecule (4B2AEAB) and its derivatives is showing high chemical reactivity and low kinetic stability

TABLE-8b  
COMPARISON OF NLO PARAMETERS WITH FEW EXISTING ORGANIC NLO MATERIALS AND 4B2AEAB, 4B2AEAB4NP AND 4B2AEABTU

NLO materials/Parameters	$\mu$ (Debye)	$\alpha$ (esu)	$\beta$ (esu)	Ref.
4B2AEAB	8.1514	$42.9298 \times 10^{-24}$	$2.805381 \times 10^{-30}$	Present work
4B2AEAB4NP	18.9971	$65.0212186 \times 10^{-24}$	$12.73333 \times 10^{-30}$	Present work
4B2AEABTU	17.2703	$54.3673182 \times 10^{-24}$	$12.00412 \times 10^{-30}$	Present work
4DMAB4NP	6.1643	$27.9971 \times 10^{-24}$	$31.4203 \times 10^{-30}$	[32]
DCNB	1.023	—	$1.2210 \times 10^{-30}$	[63]
3AP4NP	4.5871	$16.815 \times 10^{-24}$	$8.7692 \times 10^{-30}$	[64]
HOQDNB	5.1730	$29.820 \times 10^{-24}$	$5.0563 \times 10^{-30}$	[65]
M2C4N	4.4591	$18.0037 \times 10^{-24}$	$2.1523 \times 10^{-30}$	[66]
2A4PNN	21.180	$18.5618 \times 10^{-24}$	$11.160 \times 10^{-30}$	[67]
NSP	4.7342	$10.8966 \times 10^{-24}$	$1.0953 \times 10^{-30}$	[68]
PDPHB	6.7025	$15.1083 \times 10^{-30}$	$4.6132 \times 10^{-30}$	[69]
PYPHB	1.1989	$14.2720 \times 10^{-30}$	$4.8393 \times 10^{-30}$	[70]

TABLE-9  
THEORETICALLY CALCULATED ENERGY VALUES IN THEIR GROUND STATE AT DFT METHOD (B3LYP AND B3PW91) WITH 6-31+G (d, p) LEVEL OF THEORY OF 4B2AEAB AND ITS DERIVATIVES USING WATER SOLVENT IN CPCM MODEL

Parameters/Equations	4B2AEAB		4B2AEAB4NP	4B2AEABTU
	B3LYP	B3PW91	B3LYP	B3LYP
$E_{\text{HOMO}}$ (eV)	-5.950	-5.997	-6.095	-6.049
$E_{\text{LUMO}}$ (eV)	-1.843	-1.862	-2.865	-2.068
$\Delta E_{\text{L-H}}$ (eV) = ( $E_{\text{L}} - E_{\text{H}}$ ) (17)	4.106	4.135	3.229	3.980
IP (eV) = ( $-E_{\text{HOMO}}$ ) (18)	5.950	5.997	6.095	6.049
EA (eV) = ( $-E_{\text{LUMO}}$ ) (19)	1.843	1.862	2.865	2.068
$\eta$ (eV) = ( $I - A/2$ ) (20)	2.053	2.067	1.614	1.990
$\chi$ (eV) = [ $-1/2(I + A)$ ] (21)	3.896	3.929	4.4805	4.0591
$\mu$ (eV) = ( $-\chi$ ) (22)	-3.896	-3.929	-4.4805	-4.0591
$S$ (eV <sup>-1</sup> ) = ( $1/2\eta$ ) (23)	0.243	0.483	0.3096	0.2512
$\omega$ (eV) = ( $\mu^2/2\eta$ ) (24)	3.698	3.734	6.2153	4.1391
$Q_{\text{max}}$ = ( $-\mu/\eta$ ) (25)	1.898	1.900	2.7743	2.0394

Note- I = ionization potential, A = electron affinity,  $E_{\text{H}}$  = energy of HOMO,  $E_{\text{L}}$  = energy of LUMO.

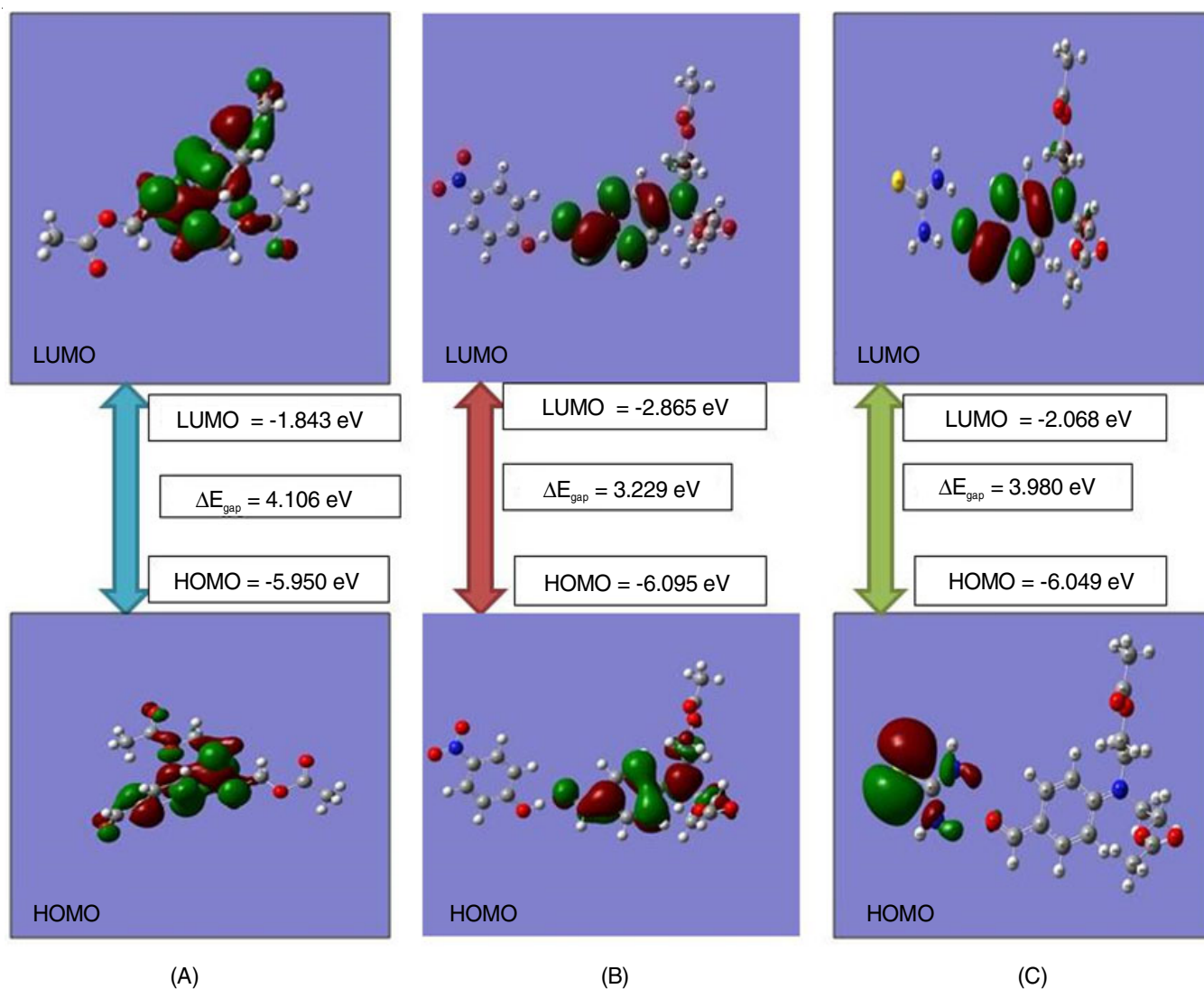


Fig. 5. Molecular orbitals and energies for the HOMO and LUMO of 4B2AEAB (A), 4B2AEAB4NP (B) and 4B2AEABTU (C) compounds in water solvent calculate at DFT/B3LYP/6-31+G (d,p) method

(a soft molecule) and displayed higher intermolecular charge transfer (ICT) [76].

**Density of states (DOS spectrum) analysis:** The molecular orbitals (HOMO and LUMO) contribution of different constituting elements present in the total system for 4B2AEAB and its derivatives, which is provided by density of state (DOS). The density of state spectrum is calculated by using GaussSum software [77] and the spectrum of 4B2AEA and its derivatives are shown in Fig. 6. From the DOS plot, it is clear that the DOS plot shows population analysis per orbitals and shows the simple view of makeup of the HOMO and LUMO in certain energy range.

**Electrostatic potential (ESP), total electron density (ED) and 2D contour map:** The 3D plot of the electrostatic potential (ESP), total electron density (ED) plot and 2D contour map plot for 4B2AEAB and its derivatives were visualized through Gauss View 5.0 program is illustrated in Fig. 7. The electrostatic potential (ESP) map is the important tool to define the charged region (electrophilic and nucleophilic sites) in the molecules or compounds in term of colour coding [78]. In present compounds, the O—H—O hydrogen bonding play an

important role in explaining the stability of the molecules. The colour code of electrostatic potential (ESP) map for 4B2AEAB, 4B2AEAB4NP and 4B2AEABTU compounds were taken from -0.0 deepest red (very negative), orange (negative), yellow (slightly negative), green (neutral), turquoise (slightly positive), light blue (positive) to +0.0 dark blue (very positive) and have 0.02 iso-value and 0.004 a.u. energy values for all the ESP of 4B2AEAB and its derivatives at DFT/B3LYP/6-31+G(d,p) level in water solvent. The oxygen atom of aldehyde group, nitro group and acetyl group of all derivatives possess negative charges and were attributed to electrophilic behaviour of the 4B2AEAB and its derivatives. Likewise, the H-atoms in the both regions surrounded by nucleophilic reactivity in all the molecule of present work. The flow of electron density in 4B2AEAB and its derivatives were represented by lines in terms of colour code.

The electrostatic potential (ESP) contour map of the 4B2AEAB and its derivatives are illustrated in Fig. 7. The red colour line represent the presence of negative charges whereas blue lines represents the positive region and green line represent the neutral region in the 4B2AEAB and its derivatives.

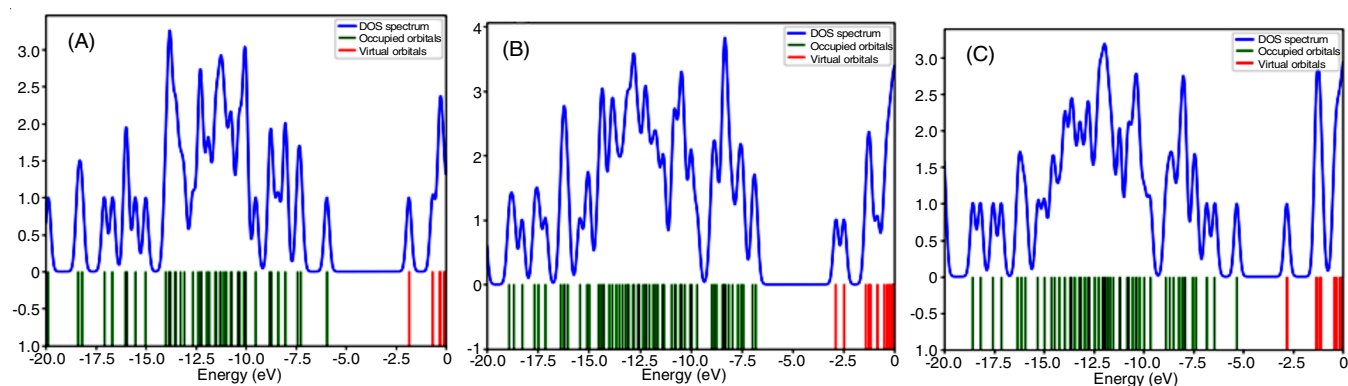


Fig. 6. Density of state (DOS) spectra of 4B2AEAB (A), 4B2AEAB4NP (B) and 4B2AEABTU (C) compounds

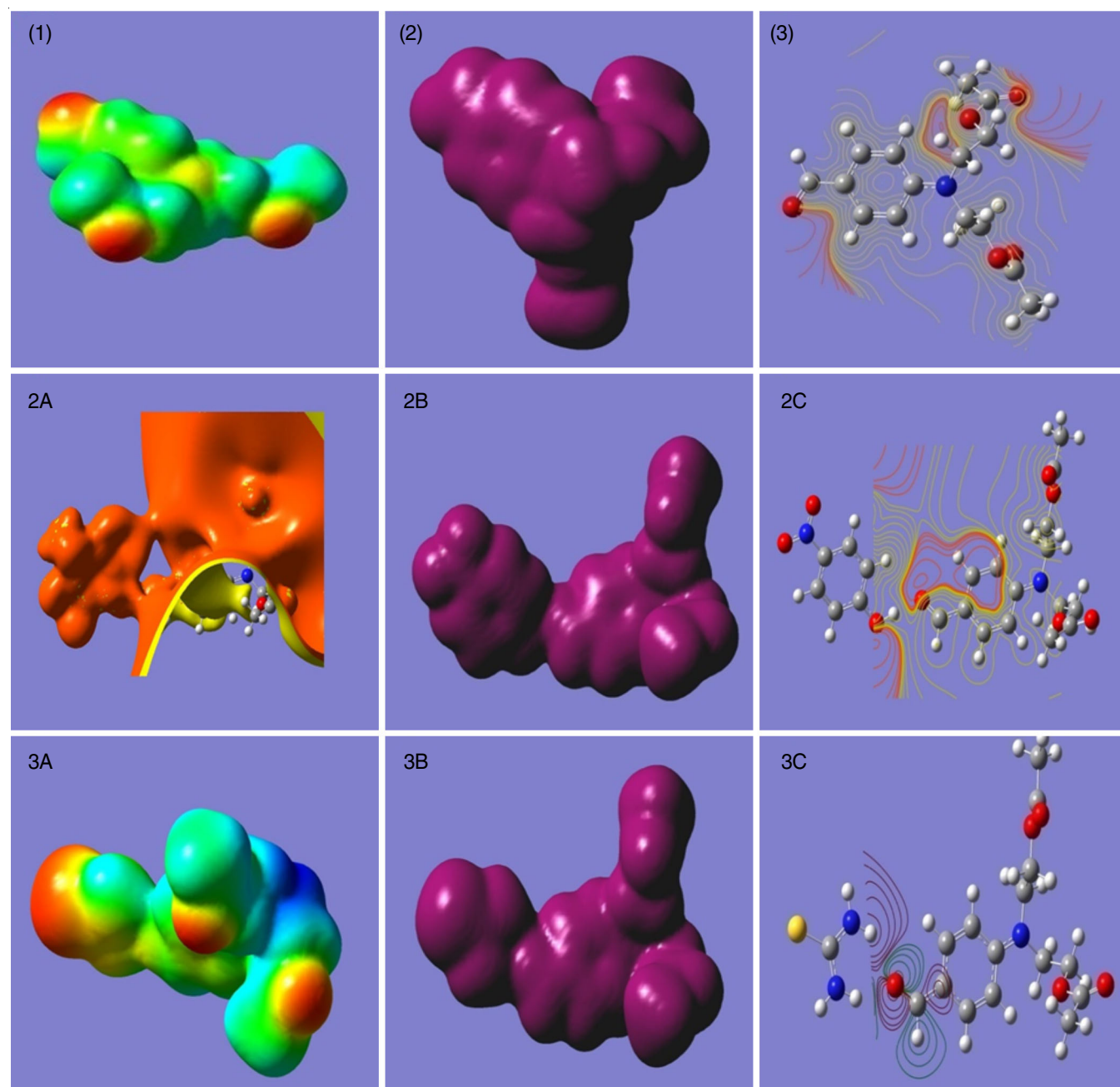


Fig. 7. ESP, electron density (ED) and 2D contour map for 4B2AEAB (1, 2 & 3), 4B2AEAB4NP (2A, 2B & 2C) and 4B2AEABTU (3A, 3B & 3C) compounds

**Mulliken atomic charges (MPA) and thermodynamic properties:** The Mulliken atomic charges of 4B2AEAB using B3LYP and B3PW91 and its derivatives (*viz.* 4B2AEAB4NP and 4B2AEABTU) were analyzed by using optimized structure at DFT/B3LYP or B3PW91/6-31+G(d,p) basis set in water solvent and are illustrated in Fig. 8.

Mulliken atomic charges of 4B2AEAB, 4B2AEAB4NP and 4B2AEABTU compounds were varied from -1.060823/-1.350507 to +0.546283/+0.566822 (at B3LYP & B3PW91 level), -0.667764 to +0.800482 (at B3LYP level) and -0.889052 to +0.553020, respectively. The atoms 1C, 3C, 11C, 13H, 15C, 20C and 31C in 4B2AEAB were positively charged and the remaining C, N, O atoms were negatively charged, whereas in 4B2AEAB4NP compound, the atoms 41C, 43C, 44C, 55H and 1C, 3C, 11C, 13H, 15C, 20C and 31C were positively charged in nitro phenol and aldehyde moiety, respectively and remaining atoms were negatively charged. In 4B2AEABTU, 41C, 43H, 44H, 46H, 47H were positively charged, while the 42N, 45N, 48S atoms of urea moiety were negatively charged.

The sum of mulliken atomic charges of the 4B2AEAB and its derivatives were estimated to be zero which confirmed the neutral charge. The results of mulliken atomic charges of the optimized structure of 4B2AEAB and its derivatives are shown in Table-10. Further, on the basis of vibrational analysis, the statistical thermodynamic functions such as entropy (S), enthalpy (H) and heat capacity ( $C_v$ ) changes of 4B2AEAB, 4B2AEAB4NP complex and 4B2AEABTU compounds were obtained from the theoretical harmonic frequencies and are calculated by computing the following equations implemented in Gaussian program [79,80]. The thermal energy (E) (internal) could be calculated using the equation given as:

$$E = Nk_B T^2 \left( \frac{\partial \ln q}{\partial T} \right)_v \quad (26)$$

The heat capacity ( $C_v$ ) could be calculated using following equation given as:

$$C_v = \left( \frac{\partial E}{\partial T} \right)_{N,v} \quad (27)$$

TABLE-10  
MULLIKEN ATOMIC CHARGES OF 4B2AEAB, 4B2AEABNP AND 4B2AEABTU

Atoms	4B2AEAB/ B3LYP	4B2AEAB/ B3PW91	Atoms	4B2AEAB4NP/ B3LYP	Atoms	4B2AEABTU/ B3LYP
1C	0.340124	0.463190	1C	0.235148	1C	0.086975
2C	-0.778038	-1.350507	2C	-0.667764	2C	-0.889052
3C	0.344823	0.366272	3C	0.455696	3C	0.320257
4C	-1.060823	-0.474383	4C	-0.361205	4C	-0.936544
5C	-0.022348	0.454702	5C	0.416705	5C	0.080285
6C	0.141297	-0.380374	6C	-0.360867	6C	0.178494
11C	0.202351	0.030521	11C	0.372824	11C	0.402624
12O	-0.455068	-0.478524	12O	-0.508601	12O	-0.455497
13H	0.150775	0.134772	13H	0.135698	13H	0.164531
14C	-0.206749	-0.267279	35N	0.084521	35N	-0.031532
15C	0.074178	-0.318866	20C	0.651450	20C	0.553020
20C	0.546283	0.566822	41C	0.306676	31C	0.498827
21C	-0.501832	-0.542460	42C	-0.083069	38O	-0.301267
25C	-0.147533	-0.202270	43C	0.047888	39O	-0.483768
26C	-0.116291	0.005433	44C	0.800482	41C	0.016020
31C	0.496510	0.470060	45C	-0.282862	42N	-0.683919
32C	-0.435581	-0.527234	46C	-0.253261	43H	0.310576
35N	-0.014756	0.148860	51O	-0.129931	44H	0.460156
36O	-0.318652	-0.217802	52N	-0.237967	45N	-0.616749
37O	-0.487564	-0.512555	53O	-0.125422	46H	0.336749
38O	-0.305580	-0.243523	54O	-0.120573	47H	0.327289
39O	-0.486664	-0.503521	55H	0.468001	48S	-0.200822

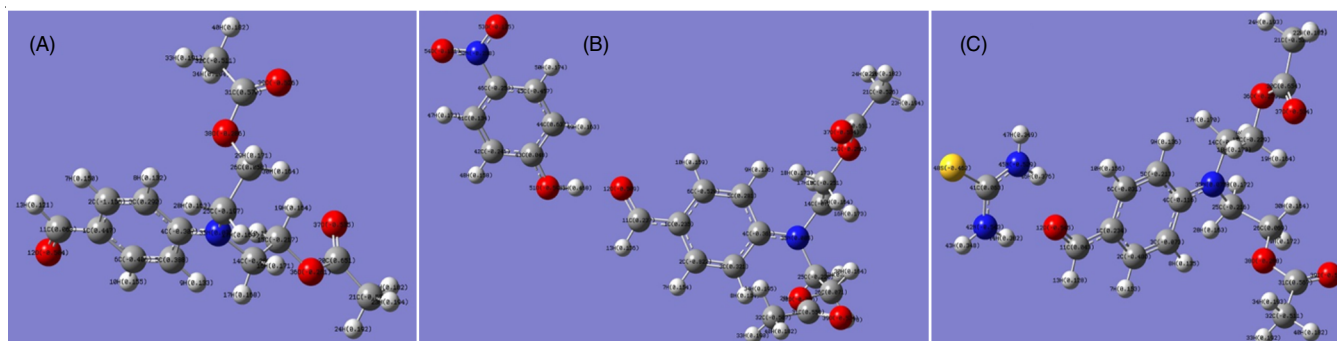


Fig. 8. Mulliken atomic charges of 4B2AEAB (A), 4B2AEAB4NP (B) and 4B2AEABTU (C) calculated at DFT/B3LYP/6-31+G (d, p) level in water solvent

TABLE-11a  
THEORETICALLY COMPUTED ROTATIONAL CONSTANT (GHz), ZPVE (Kcal mol<sup>-1</sup>), THERMAL ENERGY (Kcal mol<sup>-1</sup>), HEAT CAPACITY (Cal mol<sup>-1</sup> Kelvin<sup>-1</sup>) AND ENTROPY (Cal mol<sup>-1</sup> Kelvin<sup>-1</sup>) OF THE TITLE MOLECULE (4B2AEAB), 4B2AEAB4NP COMPLEX AND 4B2AEABTU COMPLEX

Parameters	4B2AEAB		4B2AEAB4NP/	4B2AEABTU/
	B3LYP	B3PW91	B3LYP	B3LYP
Rotational constant (GHz)				
x	0.26588	0.26811	0.18519	0.22251
y	0.19175	0.19344	0.03753	0.06594
z	0.13027	0.13163	0.03403	0.05540
ZPVE (Kcal/mol)	203.94043	204.41123	271.96050	243.08194
H (Kcal/mol)	217.857	218.376	291.945	261.289
C <sub>v</sub> (Cal/mol-Kelvin)	78.315	78.222	113.068	100.466
S (Cal/mol-Kelvin)	169.890	173.054	225.668	211.603

Similarly, entropy (s) could be calculated using the following equation by using vibrational (q<sub>v</sub>), translational (q<sub>t</sub>), rotational (q<sub>r</sub>) and electronic (q<sub>e</sub>) partition functions given as:

$$S = Nk_B + Nk_B \ln \left( \frac{q(V, T)}{N} \right) + Nk_B T \left( \frac{\partial \ln q}{\partial T} \right)_V \quad (28)$$

The thermodynamic properties like thermal energy (E), heat capacity (C<sub>v</sub>) and entropy (S) of 4B2AEAB, 4B2AEAB4NP and 4B2AEABTU compounds were calculated at constant pressure 1 atm and temperature 298.15 Kelvin at DFT/B3LYP/6-31+G(d, p) level of theory in water solvent using CPCM model and results are given in Table-11a. The order of highest value of E, C<sub>v</sub>, S, ZPVE are 4B2AEAB4NP > 4B2AEABTU > 4B2AEAB, respectively.

On the basis of vibrational analysis and statistical thermodynamics, the thermodynamics functions such as heat capacity (C<sub>v</sub>), enthalpy (E) and entropy (S) changes were calculated from 100 K to 1000 K at DFT/B3LYP/6-31+G(d,p) level of theory in water solvent using CPCM model for the title molecule (4B2AEAB) were obtained from the theoretical calculation of harmonic wavenumbers (cm<sup>-1</sup>) and are presented in Table-11b. From Table-11b, it is clearly observed that these thermodynamic functions (enthalpy, heat capacity, entropy) are increasing with temperature in the range 100-1000 K and the corresponding fitting factor (R<sup>2</sup>) for enthalpy (E), heat capacity (C<sub>v</sub>) and entropy (S) are 0.971, 0.962 and 0.995, respectively. The correlation between thermodynamic properties and temperature are illustrated in Figs. 9 and 10 and the graph equations are as follows:

For enthalpy (H):  $y = 0.114x + 182.3$  (R<sup>2</sup> = 0.971)  
and coefficient (r) = 0.9855

For heat capacity (C<sub>v</sub>):  $y = 0.154x + 26.13$  (R<sup>2</sup> = 0.962)  
and coefficient (r) = 0.9811

For entropy (S):  $y = 0.223x + 72.59$  (R<sup>2</sup> = 0.995)  
and coefficient (r) = 0.9975

The data of all the thermodynamic properties can be used to theoretically compute the other thermodynamic energies according to relationships of thermodynamic functions and estimated direction of chemical reactions according to the 2<sup>nd</sup> law of thermodynamics in thermochemical field [81].

**in silico Biological evaluation (Lipinski 'rule of five') and ADMET investigation results:** Table-12a shows a clear view

TABLE-11b  
THERMODYNAMIC FUNCTIONS AT DIFFERENT TEMPERATURE OF THE TITLE MOLECULE (BAEAB) CALCULATED AT DFT/B3LYP/6-31+G (d, p) IN WATER SOLVENT USING CPCM MODEL

Temperature (K)	Enthalpy (H) (Kcal mol <sup>-1</sup> )	Heat capacity (C <sub>v</sub> ) (Cal mol <sup>-1</sup> Kelvin <sup>-1</sup> )	Entropy (S) (Cal mol <sup>-1</sup> Kelvin <sup>-1</sup> )
100	204.185	29.041	87.307
200	208.138	50.227	115.247
300	214.299	73.178	140.723
400	222.742	95.250	165.431
500	233.234	113.948	189.208
600	245.410	129.002	211.727
700	258.936	141.109	232.861
800	273.559	151.028	252.638
900	289.088	159.318	271.153
1000	305.381	166.354	288.522

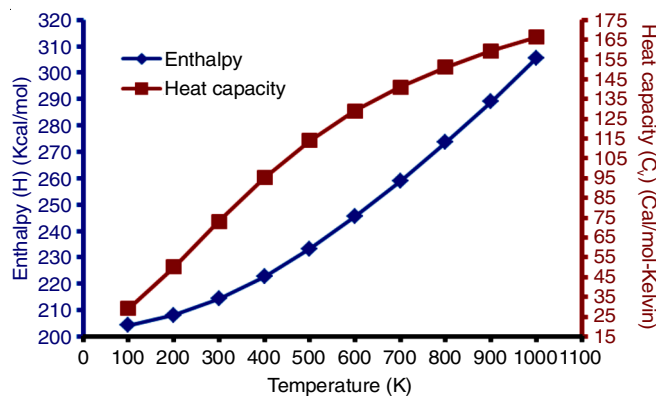


Fig. 9. Correlation graphics of enthalpy (H) and heat capacity (C<sub>v</sub>) and temperature (K) for 4B2AEAB

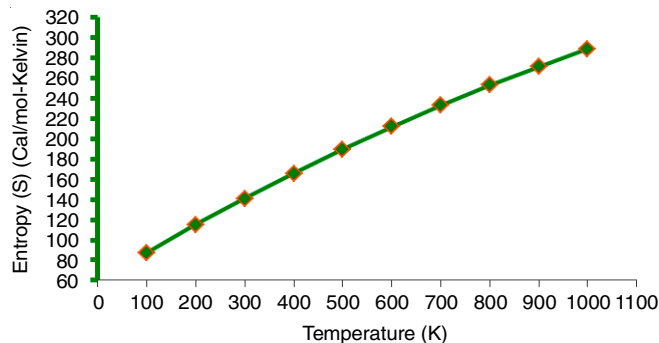


Fig. 10. Correlation graphics of entropy (S) and temperature (K) for 4B2AEAB

TABLE-12a  
*in silico* PHYSICO-CHEMICAL PHARMACOKINETIC PARAMETERS IMPORTANT FOR GOOD ORAL BIOAVAILABILITY AND BIOACTIVITY PREDICTION OF 4B2AEAB, 4B2AEABNP AND 4B2AEABTU WERE CALCULATED FROM MOLINSPIRATION FREE ONLINE SERVER

Physico-chemical properties	4B2AEAB	4B2AEAB4NP	4B2AEABTU
miLog P <sup>a</sup>	1.97	0.40	-1.63
TPSA <sup>b</sup> (Å)	72.92	122.08	105.07
MW <sup>c</sup>	299.32	432.42	369.44
No. HBA <sup>d</sup>	6	8	8
No HBD <sup>e</sup>	0	2	5
nRotB <sup>f</sup>	10	11	13
Volume <sup>g</sup>	272.08	390.42	338.10
nVotions <sup>h</sup>	0	0	0
%ABS <sup>i</sup>	83.84%	66.63%	72.75%
Log S <sup>j</sup> (Mol/L)	-2.42 (Soluble)	-5.32 (M. soluble)	-3.38 (Soluble)
Bioavailability score	0.55	0.55	0.55
Bioactivity	Values	Values	Values
GPCR ligand	-0.19	-0.16	-0.23
Ion channel modulator	-0.10	-0.11	-0.23
Kinase inhibitor	-0.17	-0.20	-0.14
Nuclear receptor ligand	-0.01	-0.08	-0.2
Protease inhibitor	-0.30	-0.13	-0.05
Enzyme inhibitor	-0.09	-0.13	-0.07

of drug-likeness properties of rationally designed 4B2AEAB, 4B2AEAB4NP and 4B2AEABTU compounds. The values of physico-chemical properties of these compounds could be obeying the Lipinski rule of five (RO5) without any violation, indicating that all the studies compounds could be orally active drugs in human because Lipinski RO5 [82] stated that the any molecule will likely to be active if (i) MW ≤ 500, (ii) log P ≤ 5, (iii) number of hydrogen bond donor (HBD) ≤ 5 and (iv) no. HBA ≤ 10. It is clear from Table-12a, that all these compounds exhibited a good percent absorption (%ABS) ranging from 66.63% to 83.84% and were found to be non-toxic in nature. A parameter used to calculate aqueous solubility is log S (S in mol/L). The solubility values of these compounds ranged from -2.42 mol/L to -5.32 mol/L. The topological polar surface area (TPSA) of these compounds have value below 160 Å, the entire molecule confirm that absorption of drug. The TPSA used to calculate the %ABS is equal to [109-(0.345 × TPSA)] [83]. All the physico-chemical properties of these compounds were calculated from Molinspiration free online server [84] and SwissADME server [85].

The bioactivity such as GPCR (G-protein coupled receptor) ligand, ion channel modulator, kinase inhibitor, nuclear receptor ligand, protease and enzyme inhibitor properties of the 4B2AEAB and derivatives were calculated from Molinspiration free online server [84] and results of bioactivity score illustrated in Table-12a and bioactivity score graph is shown in Fig. 11. The bioactivity are measured by bioactivity score categorized under three deferent conditions (i) if bioactivity score more than 0.00, having considerable bioactivity, (ii) if bioactivity score 0.5 to 0.00, having moderate biological activity, (iii) if bioactivity score is less than -0.50, having inactivity [86]. The results of the present study are fulfilled that 4B2AEAB and its derivatives are biologically active and have physiological effects.

The absorption, distribution, metabolism, excretion and toxicity (ADMET) properties of all the three compounds are

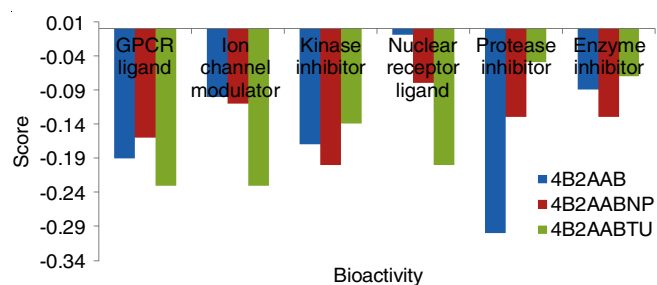


Fig. 11. Bioactivity score graphics of 4B2AEAB, 4B2AEAB4NP and 4B2AEABTU compounds

illustrated in Table-12b and 12c. The entire properties like ADMET are predicted from SwissADME server [85] and preADMET server [87].

From Table-12b and 12c, it is clear that the gastrointestinal absorption (GI) of 4B2AEAB is high while 4B2AEAB4NP and 4B2AEABTU is low because 30% ABS standard value for gastrointestinal absorption. The skin permeability (log K<sub>p</sub> in cm/s) high for 4B2AEAB, 4B2AEAB4NP and 4B2AEABTU were -7.17, -7.03 and -8.23 cm/s, which shows a high permeability in the skin because standard value for skin permeability log K<sub>p</sub> is -2.5 cm/s. The 4B2AEAB and its derivatives are not blood brain barrier (BBB) permeant and from Fig. 12, a yellow coloured point shown in “boiled egg” show the molecule-1 (4B2AEAB) is not passively transferred through the blood brain barrier (BBB).

In present study, compound 4B2AEAB in Fig. 12 pointed in the “boiled egg” white is molecule predicted to be passively absorbed by the gastrointestinal tract but compound-2 (4B2AEAB4NP) and compound-3 (4B2AEABTU) are not permeate by gastrointestinal tract. Where compound-1 (4B2AEAB) and compound-3 (4B2AEABTU) (shown in red dot in “boiled egg”, Fig. 12) are not effluated from the central nervous system (CNS) by the P-glycoprotein but in case of

TABLE-12b  
 ABSORPTION, DISTRIBUTION, METABOLISM AND EXCRETION (ADME) PROPERTIES OF 4B2AEAB, 4B2AEABNP AND 4B2AEABTU WERE CALCULATED FROM preADMET SERVER AND swissADME SERVER

Properties	4B2AEAB	4B2AEAB4NP	4B2AEABTU
GI Absorption	High	Low	Low
BBB Permeant	No	No	No
BBB value	0.0191	0.1132	0.03440
Buffer solubility (Mg/L)	13.3211	0.22247	2.54582
Caco2 (nm/sec)	24.564	5.7332	20.0203
P-GP Substrate	No	Yes	No
CYP1A2 inhibitor	Yes	No	No
CYP2C19 inhibitor	No	Yes	No
CYP 2C9 inhibitor	No	No	No
CYP2D6 inhibitor	No	No	No
CYP3A4 inhibitor	No	No	No
Log K <sub>p</sub> (SP) (cm/s)	-7.17	-7.03	-8.23
HIA (%)	96.5216	84.5418	85.1513
MDCK (nm/sec)	138.162	33.7056	46.9751
P. P. Binding (%)	70.3557	92.1583	96.6583
PWS (Mg/L)	1228.06	56.533	186.994

TABLE-12c  
 TOXICITY PROFILE 4B2AEAB, 4B2AEAB4NP AND 4B2AEABTU COMPLEX WERE CALCULATED FROM preADMET SERVER

Properties	4B2AEAB	4B2AEAB4NP	4B2AEABTU
Acute algae toxicity	0.1141	0.9163	0.01629
Ames test	Mutagen	Mutagen	Mutagen
Carcinogenicity (mouse)	Negative	Negative	Negative
Carcinogenicity (Rat)	Negative	Negative	Negative
Acute daphnia toxicity	0.46013	0.05035	0.2241
<i>in vitro</i> hERG inhibition	M. risk	M. risk	M. risk
<i>in vitro</i> Ames test TA100 (+S9) strain (Rat Liver)	Negative	Positive	Positive
<i>in vitro</i> Ames test TA100 (-S9) strain	Negative	Negative	Negative
<i>in vitro</i> Ames test TA1535 (+S9) strain (Rat Liver)	Negative	Negative	Negative
<i>in vitro</i> Ames test TA1535 (-S9) strain	Negative	Negative	Negative

Note: hERG = Human Ether-a-go-go-Related Gene (KCNH<sub>2</sub> gene), Positive = Positive in test, Negative = Negative in test, M. risk = Medium risk.

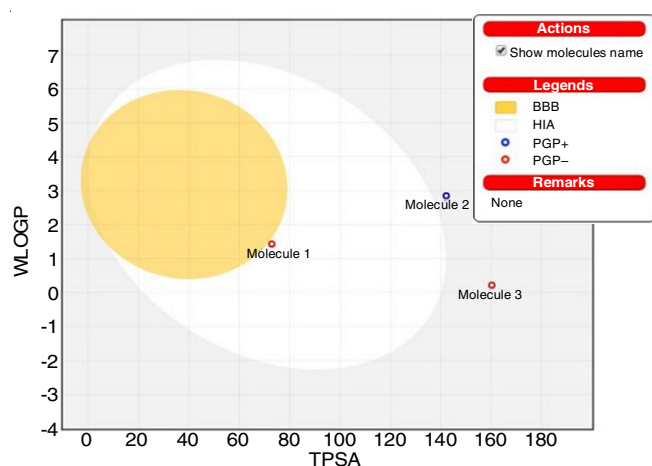


Fig. 12. Test and illustrative use of “Boiled Egg”: 4B2AEAB (molecule-1) represented by red circle (well absorbed in human intestine and not effluated from CNS by P-GPs) and 4B2AEAB4NP (molecule-2) represented by blue colour (positively effluated from CNS by P-GPs) and 4B2AEABTU (molecule-2) not effluated from CNS by P-glycoprotein

compound-2 (4B2AEAB4NP) are shown in blue dot in the “boiled egg” is effluated from CNS by the P-glycoprotein. The caco-2 cells permeability are making out from human colon adenocarcinoma and posses multiple drug transport pathway

through the intestinal epithelium at pH 7.4 [88]. Here, the 4B2AEAB, 4B2AEAB4NP and 4B2AEABTU compounds are middle permeability. Also, we discussed about the cytochrome P450 (CYP) super family of enzymes key player in oxidize steroids, fatty acids and xenobiotics and are important for the clearance of various compounds, as well as for hormone synthesis and drugs elimination through metabolic biotransformation [89]. The cytochrome P450 super family contains five major isoforms (CYP1A2, CYP2C19, CYP2C9, CYP2D6 and CYP3A4). Here 4B2AEAB only inhibits the CYP1A2 isoenzymes and shows a major cause of pharmacokinetics related drug-drug interactions leading to toxic or other unwanted adverse effects due to lower clearance and accumulation of the drug or its metabolites and the 4B2AEAB compound not inhibited the remaining isoenzymes of super family. The 4B2AEAB4NP and 4B2AEABTU compounds are easily eliminated and cleared through metabolic biotransformation due to both the complex are not inhibited the any isoenzymes of super family of cytochrome P450. The prediction of human intestinal absorption (HIA) is very important for discovery of potential drug candidate. The predicted data of HIA is the sum of absorption and bioavailability evaluated from ratio of excretion or cumulative excretion in urine, bile and feces at pH 7.4 [90]. In the present study, the 4B2AEAB and its derivatives are well absorbed comp-

ounds because the values are 96.5216, 84.5418 and 85.1513% at pH 7.4, found in acceptable range (0-20% poorly absorbed compounds, 20-70% moderately absorbed compounds, 70-100% well absorbed compounds) [91]. The phenomena of plasma protein bonding with any drug influence the drug action but also its deposition and efficacy. Generally, unbound drug is available for diffusion or transport across the cell membrane and also for interaction with physiological target. In the present study, 4B2AEAB compound easily diffuse or transport the cell membrane and also for interaction with target. The value of PPB percentage for 4B2AEAB compound is 70.3557% (chemical weakly bound have value less than 90%), while the other compounds (4B2AEAB4NP and 4B2AEABTU) were strongly bounded with PPB because both compound have plasma protein binding value of 92.1583% and 96.6583% (reference value: more than 90% the molecule bound strongly with PPB), respectively.

The toxicity profile of 4B2AEAB and its derivatives are presented in the Table-12c. From Table-12c, it is clear that 4B2AEAB and its derivatives are mutagen by Ames test. The 4B2AEAB and its derivatives results shows negative, so that the entire molecule produce carcinogenicity in mice and rat. The preADMET predict toxicity to TA100 and TA1535 strain (+S9 with rat liver and -S9 strain without rat liver) which are often used in Ames test. All the result of Ames test for entire compounds in present study is in negative (no change of population *versus* blank plate). In the case of 4B2AEAB4NP and 4B2AEABTU compounds show positive Ames test for TA100 (+S9 strain rat liver) strain (means change of population, more than double of blank plate's change). The hERG K<sup>+</sup> channel is responsible for electrical activity of heart that coordinates the heart's beating; appear to be the molecular target responsible for the cardiac toxicity of wide range of therapeutic drugs [92]. In the present study, the entire molecule shows medium risk for hERG K<sup>+</sup> channel. The *in silico* study provides the cardiac toxicity of drugs in the early stage of drug discovery. The results of this *in silico* bioactivity score prediction, physico-chemical study and ADMET prediction analysis suggest that the computational designed 4B2AEAB, 4B2AEAB4NP and 4B2AEABTU follow the criteria for orally active drugs and thus represent a pharmacological active framework that should be considered on progressing further potential hits [93].

## Conclusion

In conclusion, a novel 4-*bis*[2-(acetyloxy)ethyl]amino]-benzaldehyde (4B2AEAB), hydrogen bonded structure and D- $\pi$ -A charge transfer type organic complex of 4-*bis*[2-(acetyloxy)ethyl]amino]-benzaldehyde-4-nitrophenol (4B2AEAB4NP) and 4-*bis*[2-(acetyloxy)ethyl]amino]benzaldehyde-thiourea (4B2AEABTU) complex have been rationally designed and structure was optimized by using DFT/B3LYP and DFT/B3PW91 method with 6-31+G(d,p) basis set in water solvent using CPCM model. The calculated vibrational wavenumbers (cm<sup>-1</sup>) and spectra agreed with the experimental FT-IR wavenumbers. The global minimum energy between the different functional shows the difference in optimization between the same and the different solvents. The magnetic properties of the 4B2AEAB were observed and calculated chemical shift of <sup>1</sup>H & <sup>13</sup>C NMR

were compared with experimental chemical shift. The net charge distributions on the 4B2AEAB molecule were calculated by Mulliken population analysis. The electrostatic potential (ESP) map, total electron density (ED) and 2D contour map showed that the negative potential sites (electrophilic attacks) are on the electronegative atoms N and O atoms (intramolecular H-bond sites) as well as the positive potential (nucleophilic attacks) sites are around the intermolecular bond sites and H atoms of the 4B2AEAB, 4B2AEAB4NP and 4B2AEABTU complexes. The ESP plots revealed the possible reaction sites of 4B2AEAB and its derivatives. The local chemical reactivity descriptors (Fukui function analysis, local softness and local philicity analysis) were calculated for the 4B2AEAB. The natural bond orbital (NBO) analysis revealed that the delocalization and hyperconjugation interactions, intra molecular charge transfer and stabilization energies of the title molecule. The theoretical UV-visible spectral analysis of 4B2AEAB and its derivatives in gas phase and solvent phase has also provided insight into the  $\lambda_{\text{max}}$ , excitation energy oscillator strength and molecular orbital assignment and predicted mainly the  $\pi \rightarrow \pi^*$  type transitions which are intramolecular charge transfer type. The non-linear optical (NLO) behaviour of 4B2AEAB and H-bonded and D- $\pi$ -A type 4B2AEAB4NP and 4B2AEABTU complex were investigated by the analysis of dipole moment ( $\mu$ ), polarizability ( $\alpha$ ), anisotropy of polarizability ( $\Delta\alpha$ ), first-order hyperpolarizability ( $\beta$ ) and second-order hyperpolarizability  $\langle\gamma\rangle$  using the DFT/B3LYP/6-31+G(d, p) method in water solvent using CPCM model. The first-order hyperpolarizability ( $\beta$ ) and second-order hyperpolarizability ( $\gamma$ ) value of 4B2AEAB, 4B2AEAB4NP complex and 4B2AEABTU complex were  $2.80538 \times 10^{-30}$  esu,  $12.73333 \times 10^{-30}$  esu,  $12.00412 \times 10^{-30}$  esu and  $-2.05599 \times 10^{-36}$  esu,  $-8.02090806 \times 10^{-36}$  esu,  $-5.52491331 \times 10^{-36}$  esu, respectively, which is almost more time higher than urea and show good agreement with organic NLO active materials. The comparative analysis between temperature and statistical thermodynamic properties are also obtained for the 4B2AEAB. It was seen that the enthalpy, heat capacity and entropy increase with the increasing temperature (100 K to 1000 K) owing to the intensities of the molecular vibrations increase with increasing temperature (100 to 1000 K). The *in silico* bioactivity score prediction, pharmacokinetic analysis and ADMET parameter analysis for the title molecule and its derivatives has been shown that these compounds have good oral drug like properties and all these compounds not have Lipinski rule of five violations and could developed as good oral drug candidates. Finally, from this study, it is clear that 4B2AEAB and its derivatives (4B2AEAB4NP and 4B2AEABTU) have superior non-linear optical (NLO) properties than urea and some organic NLO material and also have pharmaceutical importance. Thus, it can be used in photonic communication devices and used as oral drug for future prospective in the field of pharmaceutical industry.

## ACKNOWLEDGEMENTS

The authors are thankful to the Department of Chemistry, University of Lucknow, Lucknow, India, for providing facilities to pursue this research work.

## CONFLICT OF INTEREST

The authors declare that there is no conflict of interests regarding the publication of this article.

## REFERENCES

- P. Vijayakumar, G.A. Babu and P. Ramasamy, *Mater. Res. Bull.*, **47**, 957 (2012); <https://doi.org/10.1016/j.materresbull.2012.01.011>
- M. Samoc, A. Samoc, B. Luther-Davies, M.G. Humphrey and M.-S. Wong, *Opt. Mater.*, **21**, 485 (2003); [https://doi.org/10.1016/S0925-3467\(02\)00187-8](https://doi.org/10.1016/S0925-3467(02)00187-8)
- A.M. Petrosyan, *J. Cryst. Phys. Chem.*, **1**, 33 (2010).
- Y. Gao, Q. Chang, H. Ye, W. Jiao, Y. Song, Y. Wang and J. Qin, *Appl. Phys. B*, **88**, 255 (2007); <https://doi.org/10.1007/s00340-007-2687-6>
- A.J. Kiran, D. Udayakumar, K. Chandrasekharan, A.V. Adhikari and H.D. Shashikala, *J. Phys. At. Mol. Opt. Phys.*, **39**, 3747 (2006); <https://doi.org/10.1088/0953-4075/39/18/005>
- A. Ronchi, T. Cassano, R. Tommasi, F. Babudri, A. Cardone, G.M. Farinola and F. Naso, *Synth. Met.*, **139**, 831 (2003); [https://doi.org/10.1016/S0379-6779\(03\)00274-1](https://doi.org/10.1016/S0379-6779(03)00274-1)
- C. Li, L. Zhang, M. Yang, H. Wang and Y. Wang, *Phys. Rev. A*, **49**, 1149 (1994); <https://doi.org/10.1103/PhysRevA.49.1149>
- W. Sun, M.M. McKerns, C.M. Lawson, G.M. Gray, C. Zhan and D. Wang, *Proc. SPIE Int. Soc. Opt. Eng.*, **4106**, 280 (2000); <https://doi.org/10.1117/12.408515>
- M. Kitazawa, R. Higuchi, M. Takahashi, T. Wada and H. Sasabe, *Appl. Phys. Lett.*, **64**, 2477 (1994); <https://doi.org/10.1063/1.111602>
- W.S. Wang, M.D. Aggarwal, J. Choi, T. Gebre, A.D. Shields, B.G. Penn and D.O. Frazier, *J. Cryst. Growth*, **198-199**, 578 (1999); [https://doi.org/10.1016/S0022-0248\(98\)01041-0](https://doi.org/10.1016/S0022-0248(98)01041-0)
- M. Jazbinsek, L. Mutter and P. Gunter, *IEEE J. Sel. Top. Quantum Electron.*, **14**, 1298 (2008); <https://doi.org/10.1109/JSTQE.2008.921407>
- J.M. Rivera, H. Reyes, A. Cortes, R. Santillan, P.G. Lacroix, C. Lepetit, K. Nakatani and N. Farfán, *Chem. Mater.*, **18**, 1174 (2006); <https://doi.org/10.1021/cm051589+>
- B.B. Ivanova and M. Spitteller, *J. Phys. Chem. A*, **114**, 5099 (2010); <https://doi.org/10.1021/jp1002758>
- A.P. Menezes, A. Jayarama and S.W. Ng, *J. Cryst. Growth*, **402**, 130 (2014); <https://doi.org/10.1016/j.jcrysgro.2014.04.026>
- P. Salek, O. Vahtras, T. Helgaker and H. Ågren, *J. Chem. Phys.*, **117**, 9630 (2002); <https://doi.org/10.1063/1.1516805>
- L.M. Hauptert and G.J. Simpson, *Ann. Rev. Phys. Chem.*, **60**, 345 (2009); <https://doi.org/10.1146/annurev.physchem.59.032607.093712>
- R. Zalesny, I.W. Bulik, W. Bartkowiak, J.M. Luis, A. Avramopoulos, M.G. Papadopoulos and P. Krawczyk, *J. Chem. Phys.*, **133**, 244308 (2010); <https://doi.org/10.1063/1.3516209>
- N. Islam and A.H. Pandith, *J. Mol. Model.*, **20**, 2535 (2014); <https://doi.org/10.1007/s00894-014-2535-7>
- S. van Elshocht, T. Verbiest, M. Kauranen, B.M.W. Langeveld-Voss, A. Persoons and E.W. Meijer, *J. Chem. Phys.*, **107**, 8201 (1997); <https://doi.org/10.1063/1.475223>
- A. Wojciechowski, M.M.M. Raposo, M.C.R. Castro, W. Kuznik, I. Fuks-Janczarek, M. Pokladko-Kowar and F. Bures, *J. Mater. Sci. Mater. Electron.*, **25**, 1745 (2014); <https://doi.org/10.1007/s10854-014-1793-6>
- T. Chen, Z. Sun, L. Li, S. Wang, Y. Wang, J. Luo and M. Hong, *J. Cryst. Growth*, **338**, 157 (2012); <https://doi.org/10.1016/j.jcrysgro.2011.10.023>
- P. Srinivasan, T. Kanagasekaran, N. Vijayan, G. Bhagavannarayana, R. Gopalakrishnan and P. Ramasamy, *Opt. Mater.*, **30**, 553 (2007); <https://doi.org/10.1016/j.optmat.2007.01.014>
- L.N. Wang, X.Q. Wang, G.H. Zhang, X.T. Liu, Z.H. Sun, G.H. Sun, L. Wang, W.T. Yu and D. Xu, *J. Cryst. Growth*, **327**, 133 (2011); <https://doi.org/10.1016/j.jcrysgro.2011.05.010>
- M. Prakash, M. Lydia Caroline and D. Geetha, *Spectrochim. Acta A Mol. Biomol. Spectrosc.*, **108**, 32 (2013); <https://doi.org/10.1016/j.saa.2013.01.078>
- H. Koshima, H. Miyamoto, I. Yagi and K. Uosaki, *Crystal Growth Des.*, **4**, 807 (2004); <https://doi.org/10.1021/cg034187s>
- V. Kannan, K. Thirupugalmani and S. Brahadeeswaran, *J. Mol. Struct.*, **1049**, 268 (2013); <https://doi.org/10.1016/j.molstruc.2013.06.055>
- G. Shanmugam, K. Ravi Kumar, B. Sridhar and S. Brahadeeswaran, *Mater. Res. Bull.*, **47**, 2315 (2012); <https://doi.org/10.1016/j.materresbull.2012.05.037>
- P. Asokan and S. Kalainathan, *J. Phys. Chem. C*, **121**, 22384 (2017); <https://doi.org/10.1021/acs.jpcc.7b07805>
- N. Karuppanan and S. Kalainathan, *J. Phys. Chem. C*, **122**, 4572 (2018); <https://doi.org/10.1021/acs.jpcc.7b11884>
- S. Kulshrestha and A.K. Shrivastava, *Phys. Scr.*, **94**, 025503 (2019); <https://doi.org/10.1088/1402-4896/aafbf8>
- S. Sathiyaa, M. Senthilkumar and C.R. Raja, *J. Mol. Struct.*, **1180**, 81 (2019); <https://doi.org/10.1016/j.molstruc.2018.11.067>
- S. Karthick, K. Thirupugalmani, V. Kannan, G. Shanmugam, M.K. Kumar, G. Vinitha, B. Sridhar and S. Brahadeeswaran, *J. Mol. Struct.*, **1178**, 352 (2019); <https://doi.org/10.1016/j.molstruc.2018.10.048>
- P. Pandey and R.N. Rai, *J. Mol. Struct.*, **1160**, 189 (2018); <https://doi.org/10.1016/j.molstruc.2018.02.002>
- A. Naem, I.M. Khan and A. Ahmad, *Russ. J. Phys. Chem. A*, **85**, 1840 (2011); <https://doi.org/10.1134/S0036024411100128>
- I.M. Pavlovic, S. Draguta, M.I. Fokina, T.V. Timofeeva and I.Y. Denisjuk, *Opt. Commun.*, **362**, 64 (2016); <https://doi.org/10.1016/j.optcom.2015.05.034>
- R.W.G. Wyckoff and R.B. Corey, *Z. Kristallogr.*, **81**, 386 (1932); <https://doi.org/10.1524/zkri.1932.81.1.386>
- <http://www.sigmadrich.com/united-states.html>
- M.J. Frisch, G.W. Trucks, H.B. Schlegel, G.E. Scuseria, M.A. Robb, J.R. Cheeseman, G. Scalmani, V. Barone, G.A. Petersson, H. Nakatsuji, X. Li, M. Caricato, A. Marenich, J. Bloino, B.G. Janesko, R. Gomperts, B. Mennucci, H.P. Hratchian, J.V. Ortiz, A.F. Izmaylov, J.L. Sonnenberg, D. Williams-Young, F. Ding, F. Lipparini, F. Egidi, J. Goings, B. Peng, A. Petrone, T. Henderson, D. Ranasinghe, V.G. Zakrzewski, J. Gao, N. Rega, G. Zheng, W. Liang, M. Hada, M. Ehara, K. Toyota, R. Fukuda, J. Hasegawa, M. Ishida, T. Nakajima, Y. Honda, O. Kitao, H. Nakai, T. Vreven, K. Throssell, J.A. Montgomery, Jr., J.E. Peralta, F. Ogliaro, M. Bearpark, J.J. Heyd, E. Brothers, K.N. Kudin, V.N. Staroverov, T. Keith, R. Kobayashi, J. Normand, K. Raghavachari, A. Rendell, J.C. Burant, S.S. Iyengar, J. Tomasi, M. Cossi, J.M. Millam, M. Klene, C. Adamo, R. Cammi, J. W. Ochterski, R. L. Martin, K. Morokuma, O. Farkas, J.B. Foresman and D.J. Fox, Gaussian 09, Revision A.02, Gaussian, Inc., Wallingford CT (2016).
- E. Frich, H. P. Hratchian, R. D. Dennington II, T. A. Keith, John Millam, B. Nielsen, A. J. Holder and J. Hiscoks, Gaussian Inc.: GaussView Version 5.0.8 (2009).
- M.H. Jamroz, Vibrational Energy Distribution Analysis: VEDA 4 Program, Warsaw, Poland (2004).
- J.P. Merrick, D. Moran and L. Radom, *J. Phys. Chem. A*, **111**, 11683 (2007); <https://doi.org/10.1021/jp073974n>
- M.J. Frisch, J.A. Pople and J.S. Binkley, *J. Chem. Phys.*, **80**, 3265 (1984); <https://doi.org/10.1063/1.447079>
- R. Ditchfield, *Mol. Phys.*, **27**, 789 (1974); <https://doi.org/10.1080/00268977400100711>
- J. Pratt, J. Hutchinson and C.L. Klein Stevens, *Acta Cryst.*, **67C**, o487 (2011); <https://doi.org/10.1107/S0108270111041825>
- R.M. Silverstein, G.C. Basseler and C. Morill, Spectroscopic Identification of Organic Compounds, Wiley: New York, edn 4 (1981).
- G. Varsanyi, Vibrational Spectra of Benzene Derivatives, Academic Press: New York (1969).

47. N. Sundaraganesan, S. Ilakiamani, P. Subramani and B.D. Joshua, *Spectrochim. Acta A Mol. Biomol. Spectrosc.*, **67**, 628 (2007); <https://doi.org/10.1016/j.saa.2006.08.020>
48. V. Krishnakumar and R. Ramasamy, *Spectrochim. Acta A Mol. Biomol. Spectrosc.*, **61**, 2526 (2005); <https://doi.org/10.1016/j.saa.2004.08.027>
49. N. Puviarasan, V. Arjunan and S. Mohan, *Turk. J. Chem.*, **26**, 323 (2002).
50. N.B. Colthup, L.H. Daly and S.E. Wilberly, *Introduction to Infrared and Raman Spectroscopy*, 3rd Edn., Academic Press, Inc. USA (1990).
51. K. Nivetha, S. Kalainathan, M. Yamada, Y. Kondo and F. Hamada, *Mater. Chem. Phys.*, **188**, 131 (2017); <https://doi.org/10.1016/j.matchemphys.2016.12.008>
52. K. Thirupugalmani, S. Karthick, G. Shanmugam, V. Kannan, B. Sridhar, K. Nehru and S. Brahadeeswaran, *Opt. Mater.*, **49**, 158 (2015); <https://doi.org/10.1016/j.optmat.2015.09.014>
53. Y. Erdogdu, O. Unsalan and M.T. Gulluoglu, *J. Raman Spectrosc.*, **41**, 820 (2010); <https://doi.org/10.1002/jrs.2520>
54. E. Reed, R.B. Weinstock and F. Weinhold, *J. Chem. Phys.*, **83**, 735 (1985); <https://doi.org/10.1063/1.449486>
55. P.W. Ayers and R.G. Parr, *J. Am. Chem. Soc.*, **122**, 2010 (2000); <https://doi.org/10.1021/ja9924039>
56. R.G. Parr and W.J. Yang, *J. Am. Chem. Soc.*, **106**, 4049 (1984); <https://doi.org/10.1021/ja00326a036>
57. W. Yang and W.J.J. Mortier, *Am. Chem. Soc.*, **108**, 5708 (1986); <https://doi.org/10.1021/ja00279a008>
58. R.K. Roy, S. Krishnamurti, P. Geerlings and S. Pal, *J. Phys. Chem. A*, **102**, 3746 (1998); <https://doi.org/10.1021/jp973450v>
59. P.K. Chattaraj, B. Maiti and U. Sarkar, *J. Phys. Chem. A*, **107**, 4973 (2003); <https://doi.org/10.1021/jp034707u>
60. V.G. Dimitriev, G.G. Gurzadyan and D.N. Nikogosyan, *Handbook of Nonlinear Optical Crystals*, Springer: Berlin (1991).
61. M. Arivazhagan, V.P. Subhasini and R. Kavitha, *Spectrochim. Acta A Mol. Biomol. Spectrosc.*, **128**, 527 (2014); <https://doi.org/10.1016/j.saa.2014.02.093>
62. D.A. Kleinman, *Phys. Rev.*, **126**, 1977 (1962); <https://doi.org/10.1103/PhysRev.126.1977>
63. M. Arivazhagan and R. Meenakshi, *Spectrochim. Acta A Mol. Biomol. Spectrosc.*, **82**, 316 (2011); <https://doi.org/10.1016/j.saa.2011.07.055>
64. S. Panchapakesan, K. Subramani and B. Srinivasan, *J. Mater. Sci. Mater. Electron.*, **28**, 5754 (2017); <https://doi.org/10.1007/s10854-016-6247-x>
65. N. Sudharsana, V. Krishnakumar and R. Nagalakshmi, *J. Cryst. Growth*, **398**, 45 (2014); <https://doi.org/10.1016/j.jcrysgro.2014.03.051>
66. S. Karthick, K. Thirupugalmani, G. Shanmugam, V. Kannan and S. Brahadeeswaran, *J. Mol. Struct.*, **1156**, 264 (2018); <https://doi.org/10.1016/j.molstruc.2017.11.115>
67. T. Chen, Z. Sun, C. Song, Y. Ge, J. Luo, W. Lin and M. Hong, *Cryst. Growth Des.*, **12**, 2673 (2012); <https://doi.org/10.1021/cg300262t>
68. V. Kannan S. Karthick and S. Brahadeeswaran, *Z. Phys. Chem.*, **233**, 1293 (2019); <https://doi.org/10.1515/zpch-2018-1231>
69. G. Shanmugam, K. Thirupugalmani, V. Kannan and S. Brahadeeswaran, *Spectrochim. Acta A Mol. Biomol. Spectrosc.*, **106**, 175 (2013); <https://doi.org/10.1016/j.saa.2013.01.006>
70. G. Shanmugam, M.S. Belsley, D. Isakov, E. de Matos Gomes, K. Nehru and S. Brahadeeswaran, *Spectrochim. Acta A Mol. Biomol. Spectrosc.*, **114**, 284 (2013); <https://doi.org/10.1016/j.saa.2013.05.070>
71. S. Gunsekaran and R.A. Balaji, *Can. J. Anal. Sci. Spectrosc.*, **53**, 149 (2008); <https://doi.org/10.1515/znc-1999-3-405>
72. A. Kumar, A. Pandey and A. Mishra, *J. Biol. Chem. Res.*, **36 (Part-A)**, 1 (2019).
73. A. Kumar, A. Pandey and A. Mishra, *J. Biol. Chem. Res.*, **36 (Part-B)**, 1 (2019)
74. A. Pandey, A. Kumar and A. Mishra *J. Biol. Chem. Res.*, **36**, 102 (2019).
75. A. Pandey, A. Kumar and A. Mishra, *Int. J. Sci. Res. Rev.*, **8**, 2087 (2019).
76. Z. Demircioglu, A.E. Yesil, M. Altun, T. Bal-Demirci and N. Ozdemir, *J. Mol. Struct.*, **1162**, 96 (2018); <https://doi.org/10.1016/j.molstruc.2018.02.093>
77. N.M. O'boyle, A.L. Tenderholt and K.M. Langner, *J. Comput. Chem.*, **29**, 839 (2008); <https://doi.org/10.1002/jcc.20823>
78. R. Thirumurugan, B. Babu, K. Anitha and J. Chandrasekaran, *J. Mol. Struct.*, **1171**, 915 (2018); <https://doi.org/10.1016/j.molstruc.2017.07.027>
79. D.A. McQuarrie and J.D. Simon, *Molecular Thermodynamics*; University Science Books: Sausalito, CA, USA (1999).
80. J.W. Ochterski, *Thermochemistry in Gaussian* (2000); <http://www.gaussian.com/thermo/thermo.pdf>
81. R. Zhang, B. Du, G. Sun and Y. Sun, *Spectrochim. Acta A Mol. Biomol. Spectrosc.*, **75**, 1115 (2010); <https://doi.org/10.1016/j.saa.2009.12.067>
82. C.A. Lipinski, F. Lombardo, B.W. Dominy and P.J. Feeney, *Adv. Drug Deliv. Rev.*, **46**, 3 (2001); [https://doi.org/10.1016/S0169-409X\(00\)00129-0](https://doi.org/10.1016/S0169-409X(00)00129-0)
83. P. Ertl, B. Rohde and P. Selzer, *J. Med. Chem.*, **43**, 3714 (2000); <https://doi.org/10.1021/jm000942e>
84. <http://www.molinspiration.com>
85. <http://www.swissadme.ch/index.php>
86. A. Verma, *Asian Pac. J. Trop. Biomed.*, **2**, S1735 (2012); [https://doi.org/10.1016/S2221-1691\(12\)60486-9](https://doi.org/10.1016/S2221-1691(12)60486-9)
87. <http://preadmet.bmdrc.kr>
88. M. Yazdaniyan, S.L. Glynn, J.L. Wright and A. Hawi, *Pharm. Res.*, **15**, 1490 (1998); <https://doi.org/10.1023/A:1011930411574>
89. B. Testa and S.D. Kraemer, *Chem. Biodivers.*, **4**, 257 (2007); <https://doi.org/10.1002/cbdv.200790032>
90. Y.H. Zhao, J. Le, M.H. Abraham, P.J. Eddershaw, C.N. Luscombe, A. Hersey, D. Boutina, G. Beck, B. Sherborne, I. Cooper and J.A. Platts, *J. Pharm. Sci.*, **90**, 749 (2001); <https://doi.org/10.1002/jps.1031>
91. S. Yee, *Pharm. Res.*, **14**, 763 (1997); <https://doi.org/10.1023/A:1012102522787>
92. J.I. Vandenberg, B.D. Walker and T.J. Campbell, *Trends Pharmacol. Sci.*, **22**, 240 (2001); [https://doi.org/10.1016/S0165-6147\(00\)01662-X](https://doi.org/10.1016/S0165-6147(00)01662-X)
93. A. Kumar, A. Pandey and A. Mishra, *Asian J. Chem.*, **32**, 706 (2020); <https://doi.org/10.14233/ajchem.2020.22507>